Eur. Phys. J. C 38, 195–213 (2004)
Digital Object Identifier (DOI) 10.1140/epjc/s2004-02039-4

THE EUROPEAN
PHYSICAL JOURNAL C

The impact factor for the virtual photon to light vector meson transition

D.Yu. Ivanov[1,a], M.I. Kotsky[2,3], A. Papa[4]

[1] Sobolev Institute of Mathematics, 630090 Novosibirsk, Russia
[2] Budker Institute for Nuclear Physics, 630090 Novosibirsk, Russia
[3] Novosibirsk State University, 630090 Novosibirsk, Russia
[4] Dipartimento di Fisica, Università della Calabria and Istituto Nazionale di Fisica Nucleare, Gruppo collegato di Cosenza, 87036 Arcavacata di Rende, Cosenza, Italy

Received: 20 May 2004 / Revised version: 28 September 2004 /
Published online: 15 November 2004 –

Abstract. We evaluate in the next-to-leading approximation the forward impact factor for the virtual photon to light vector meson transition in the case of longitudinal polarization. We find that in the hard kinematic domain, both in the leading and in the next-to-leading approximation, the expression for the impact factor factorizes, up to power suppressed corrections, into the convolution of a perturbatively calculable hard-scattering amplitude and a meson twist-2 distribution amplitude.

1 Introduction

Diffractive processes in high-energy particle physics are of central interest in present and forthcoming experiments. Among them particularly important are those processes with a large typical momentum transfer Q^2, so-called semi-hard processes, since they allow a theoretical description to be given by perturbative QCD. The most suitable approach for such a description in the limit of high energy $\sqrt{s}$ is the BFKL approach [1], which has become widely known since the discovery at HERA of the sharp rise of the proton structure function for decreasing value of the Bjorken variable x (see, for example, [2]).

In the BFKL approach the high-energy scattering amplitudes are expressed in terms of the Green's function of two interacting reggeized gluons and of the impact factors of the colliding particles (see, for instance, [3]). The BFKL equation allows one to determine this Green's function. The impact factors depend on the process in question and must be calculated separately.

The BFKL equation was initially derived in the leading logarithmic approximation (LLA) which means summation of all terms of the type $(\alpha_s \ln(s))^n$. The most important disadvantage of LLA is that neither the scale of energy nor the argument of the QCD running coupling constant α_s are constrained in this approximation. The corresponding uncertainties related with the change of these scales diminish the predictive power of the LLA and restrict its application to the phenomenology. This is why the generalization of the BFKL approach to the next-to-leading logarithmic approximation (NLA), which means resummation of both the leading terms $(\alpha_s \ln(s))^n$ and of the terms $\alpha_s(\alpha_s \ln(s))^n$, is very important. The radiative corrections to the kernel of the BFKL equation were calculated several years ago [4–9] and the explicit form of the kernel of the equation in the NLA is known now [10, 11] for the case of forward scattering. Instead, the problem of calculating NLA impact factors has been solved so far only for colliding partons [12, 13] and for forward jet production [14], while no impact factors for colorless objects are known with the NLA accuracy.

It is clear that for a complete NLA description in the BFKL approach one needs to know the impact factors describing the transitions between colorless particles, analogously as in the DGLAP approach one should know not only the parton distributions, but also the coefficient functions.

The impact factor for the $\gamma^* \to \gamma^*$ transition is certainly the most important one from the phenomenological point of view, since it would open the way to predictions of the $\gamma^*\gamma^*$ total cross section. However, its calculation in the NLA turns out to be rather complicated and so far only partial results are available [15]. For an alternative approach to the calculation of the photon impact factor, see also [16].

In this paper we consider instead the NLA impact factor for the transition from a virtual photon γ^* to a light neutral vector meson $V = \rho^0, \omega, \phi$. As we will explain in detail below, the evaluation of this impact factor is considerably simpler than for the case of the $\gamma^* \to \gamma^*$ impact factor. Indeed, we obtained a closed analytical expression for this impact factor in the NLA. This result should help to understand more easily the main physical effects of the radiative corrections in the BFKL approach. As a matter of fact, the knowledge of the $\gamma^* \to V$ impact factor allows for

[a] e-mail: d-ivanov@math.nsc.ru

the first time to determine completely within perturbative QCD and with NLA accuracy the amplitude of a physical process, the $\gamma^*\gamma^* \to VV$ reaction. This possibility is interesting not only for theoretical reasons, since it could shed light on the correct choice of energy scales in the BFKL approach and could be used to compare different approaches such as BFKL and DGLAP, but also for the possible applications to the phenomenology. Indeed, the calculation of the $\gamma^* \to V$ impact factor is the first step towards the application of BFKL approach to the description of processes such as the vector meson electroproduction $\gamma^* p \to Vp$, being carried out at the HERA collider, and the production of two mesons in the photon collision $\gamma^*\gamma^* \to VV$ or $\gamma^*\gamma \to VJ/\Psi$, which can be studied at high-energy e^+e^- and $e\gamma$ colliders.

This paper is organized as follows. In the next section we will recall the definition of impact factor in the BFKL approach and outline the general framework of the calculation; in Sect. 3 we give a detailed derivation of the leading logarithmic approximation (LLA) impact factor; Sect. 4 is devoted to the calculation of the impact factor in the NLA; in Sect. 5 we summarize our results and draw some conclusions.

2 General framework

In the BFKL approach (see, for example, [3] for details) the scattering amplitude $(\mathcal{A})_{AB}^{A'B'}$ of the process $AB \to A'B'$, where A, B, A', B' are colorless particles, for CMS energy $\sqrt{s} \to \infty$ and fixed momentum transfer $\Delta \approx \Delta_\perp$ ($\perp$ means transverse to the initial particle momenta plane) is expressed in terms of the Mellin transform of the Green's function of two interacting reggeized gluons in the color singlet state G_ω and of the impact factors of the colliding particles $\Phi_{A\to A'}$ and $\Phi_{B\to B'}$:

$$
\begin{aligned}
&\mathrm{Im}_s\,(\mathcal{A})_{AB}^{A'B'} \\
&= \frac{s}{(2\pi)^{D-2}} \int \frac{\mathrm{d}^{D-2}q_1}{\mathbf{q}_1^2(\mathbf{q}_1-\mathbf{\Delta})^2} \int \frac{\mathrm{d}^{D-2}q_2}{\mathbf{q}_2^2(\mathbf{q}_2-\mathbf{\Delta})^2} \\
&\quad \times \Phi_{A\to A'}(\mathbf{q}_1,\mathbf{\Delta},s_0) \int_{\delta-\mathrm{i}\infty}^{\delta+\mathrm{i}\infty} \frac{\mathrm{d}\omega}{2\pi\mathrm{i}} \left[\left(\frac{s}{s_0}\right)^{\omega} G_\omega(\mathbf{q}_1,\mathbf{q}_2,\mathbf{\Delta}) \right] \\
&\quad \times \Phi_{B\to B'}(-\mathbf{q}_2,-\mathbf{\Delta},s_0), \qquad (1)
\end{aligned}
$$

where Im_s means s-channel imaginary part, the vector sign is used for denotation of the transverse components, $D = 4 + 2\varepsilon$ is the space-time dimension different from 4 to regularize both infrared and ultraviolet divergences and s_0 is the energy scale parameter. The Green's function obeys the BFKL equation generalized for non-zero momentum transfer [3]

$$
\begin{aligned}
&\omega\, G_\omega(\mathbf{q}_1,\mathbf{q}_2,\mathbf{\Delta}) \\
&= \mathbf{q}_1^2(\mathbf{q}_1-\mathbf{\Delta})^2 \delta^{(D-2)}(\mathbf{q}_1-\mathbf{q}_2) \\
&\quad + \int \frac{\mathrm{d}^{D-2}k}{\mathbf{k}^2(\mathbf{k}-\mathbf{\Delta})^2} \mathcal{K}(\mathbf{q}_1,\mathbf{k},\mathbf{\Delta}) G_\omega(\mathbf{k},\mathbf{q}_2,\mathbf{\Delta})\,, \qquad (2)
\end{aligned}
$$

where $\mathcal{K}$ is the NLA singlet kernel, and is completely defined by this equation. The definition of the NLA impact factors has been given in [3]; in the case of scattering of the particle A off a reggeized gluon with momentum q_1, for transverse momentum $\mathbf{\Delta}$ and singlet color representation in the t-channel, the impact factor has the form [12]

$$
\begin{aligned}
&\Phi_{A\to A'}(\mathbf{q}_1,\mathbf{\Delta},s_0) \\
&= \frac{\delta^{cc'}}{\sqrt{N_c^2-1}} \left[\left(\frac{s_0}{\mathbf{q}_1^2}\right)^{\frac{1}{2}\omega(-\mathbf{q}_1^2)} \left(\frac{s_0}{(\mathbf{q}_1-\mathbf{\Delta})^2}\right)^{\frac{1}{2}\omega(-(\mathbf{q}_1-\mathbf{\Delta})^2)} \right. \\
&\quad \left. \times \sum_{\{f\}} \int \frac{\mathrm{d}\kappa}{2\pi} \theta(s_\Lambda-\kappa)\mathrm{d}\rho_f \Gamma^c_{A\{f\}} \left(\Gamma^{c'}_{A'\{f\}}\right)^* \right] \\
&\quad - \frac{1}{2} \int \frac{\mathrm{d}^{D-2}k}{\mathbf{k}^2(\mathbf{k}-\mathbf{\Delta})^2} \Phi^{\mathrm{Born}}_{A\to A'}(\mathbf{k},\mathbf{\Delta},s_0) \mathcal{K}_r^{\mathrm{Born}}(\mathbf{k},\mathbf{q}_1,\mathbf{\Delta}) \\
&\quad \times \ln\left(\frac{s_\Lambda^2}{s_0(\mathbf{k}-\mathbf{q}_1)^2}\right)\,, \qquad (3)
\end{aligned}
$$

where c, c' are the color indices of the reggeized gluon in the initial and in the final state, respectively, $\omega(t)$ is the reggeized gluon trajectory in the LLA and the intermediate parameter s_Λ must be taken tending to infinity. The integration in the first term of the above equality is carried out over the phase space $\mathrm{d}\rho_f$ and over the squared invariant mass κ of the system $\{f\}$ produced in the fragmentation region of the particle A, $\Gamma^c_{A\{f\}}$ are the particle-reggeon effective vertices for this production and the sum is taken over all systems $\{f\}$ which can be produced in the NLA. The second term in (3) is the counterterm for the LLA part of the first one, so that the logarithmic dependence of both terms on the intermediate parameter $s_\Lambda \to \infty$ disappears in their sum; $\mathcal{K}_r^{\mathrm{Born}}$ is the part of the leading order BFKL kernel related to the real gluon production (see [3] for more details). It was shown in [17] that the definition (3) guarantees the infrared finiteness of the impact factors of colorless particles.

In this paper we will study in the NLA and in the forward ($\mathbf{\Delta} = 0$) case the impact factor which describes the transition of a virtual photon to a light neutral meson $\Phi_{\gamma^*\to V}$, $V = \rho^0, \omega, \phi$. To start with, let us describe the kinematics which is presented in Fig. 1. We introduce two auxiliary Sudakov vectors p_1 and p_2, such that $p_1^2 = p_2^2 = 0$

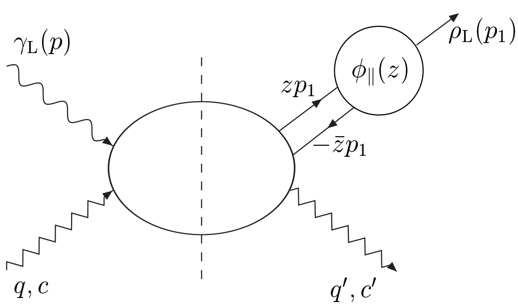

Fig. 1. The kinematics of the virtual photon to vector meson impact factor

and $2(p_1p_2) = s$. The virtual photon momentum is $p = p_1 - \zeta p_2$, where $\zeta = Q^2/s$. The large negative virtuality of the photon $p^2 = -Q^2$ introduces a hard scale in the problem and justifies the application of perturbative QCD. We denote the reggeon momenta as

$$q = \frac{\kappa + Q^2 + \mathbf{q}^{\,2}}{s} p_2 + q_\perp \,, \quad q^2 = q_\perp^2 = -\mathbf{q}^{\,2} \,,$$
$$q' = \frac{\kappa + \mathbf{q}^{\,2}}{s} p_2 + q_\perp \,, \tag{4}$$

where κ is the squared invariant mass of the intermediate state produced in the virtual photon-reggeon interaction. The component of the reggeon momentum proportional to the Sudakov vector p_1 is inessential for the analysis of the impact factor; therefore it is not included in (4). We restrict our consideration to the forward case, when the momentum transfer vector has only the longitudinal component, $q - q' = \zeta p_2$. We remark that our denotation of reggeon momenta here is slightly different from (3), since we use the symbols q and q' for the momenta of the incoming and outgoing reggeon, instead of q_1 and q_2 of (3). We assume that both the square of the reggeon transverse momentum $\mathbf{q}^{\,2}$ and the virtuality of the photon Q^2 are much larger than any hadronic scale. In what follows we will neglect all power suppressed contributions. Therefore we neglect the vector meson mass and denote the momentum of the produced vector meson by the Sudakov vector p_1.

We will show that in this kinematics the impact factor can be calculated in the collinear factorization framework [18–20] which was developed for the QCD description of hard exclusive processes. We will demonstrate by explicit calculation that the dominant helicity amplitude is a transition of the longitudinally polarized photon $\gamma_{\rm L}^*$ into the longitudinally polarized meson $V_{\rm L}$, and that both in LLA and in NLA the expression for the impact factor factorizes into the convolution[1]

$$\Phi_{\gamma_{\rm L}^* \to V_{\rm L}}(\alpha, s_0) \tag{5}$$
$$= -\frac{4\pi e_q f_V \delta^{cc'}}{N_c Q} \int_0^1 \mathrm{d}z \, T_{\rm H}(z, \alpha, s_0, \mu_{\rm F}, \mu_{\rm R}) \, \phi_\parallel(z, \mu_{\rm F})$$

of a perturbatively calculable hard-scattering amplitude, $T_{\rm H}$, and a meson twist-2 distribution amplitude, $\phi_\parallel(z)$. The distribution amplitude is defined as the vacuum-to-meson matrix element of the light-cone operator

$$\langle 0 | \bar{\Psi}(0) \gamma^\mu \Psi(y) | V_{\rm L}(p_1) \rangle_{y^2 \to 0}$$
$$= f_V \, p_1^\mu \int_0^1 \mathrm{d}z \, \mathrm{e}^{-\mathrm{i}z(p_1 y)} \, \phi_\parallel(z, \mu_{\rm F}) \,, \tag{6}$$

where $f_V \simeq 200\,\mathrm{MeV}$ is the meson decay constant; it has the meaning of the probability amplitude to find a meson in a state with minimal number of constituents – quark and antiquark – when they are separated by small transverse distances, $r_\perp \sim 1/\mu_{\rm F}$. Here $\mu_{\rm F}^2 \sim Q^2, \mathbf{q}^{\,2}$ is a factorization (or separation) scale at which soft and hard physics factorizes according to (5). The variable z corresponds to the longitudinal momentum fraction carried by the quark, for the antiquark the fraction is $\bar{z} = 1 - z$. Finally, $N_c = 3$ in (5) stands for the number of QCD colors, we introduced the ratio

$$\alpha = \frac{\mathbf{q}^{\,2}}{Q^2} \,, \tag{7}$$

and we separated the other factors for further convenience. We use the conventions of [21] for the vector meson distribution amplitude.

Equations (5) and (6) give the contribution to the impact factor of the single light quark flavor q carrying electric charge e_q. According to the neutral mesons flavor structure,

$$|\rho^0\rangle = \frac{1}{\sqrt{2}} \left(|\bar{u}u\rangle - |\bar{d}d\rangle \right) \,, \quad |\omega\rangle = \frac{1}{\sqrt{2}} \left(|\bar{u}u\rangle + |\bar{d}d\rangle \right) \,,$$
$$|\phi\rangle = |\bar{s}s\rangle \,, \tag{8}$$

e_q should be replaced by $e/\sqrt{2}$, $e/(3\sqrt{2})$ and $-e/3$ for the case of ρ^0, ω and ϕ meson production, respectively.

The hard-scattering amplitude $T_{\rm H}$ is represented as a series in the QCD running coupling constant $\alpha_{\rm s}(\mu_{\rm R})$, where the renormalization scale $\mu_{\rm R}$ is of the order of the hard scale $\mu_{\rm R}^2 \sim Q^2, \mathbf{q}^{\,2}$. The distribution amplitude is a non-perturbative function, but its dependence on the scale $\mu_{\rm F}$ is perturbative,

$$\mu_{\rm F}^2 \frac{\mathrm{d}\phi_\parallel(z, \mu_{\rm F})}{\mathrm{d}\mu_{\rm F}^2} = \int_0^1 V(z, z') \phi_\parallel(z', \mu_{\rm F}) \mathrm{d}z' \,, \tag{9}$$

and is determined by the renormalization group equation for the non-local light-cone operator in the left-hand side of (6). It is renormalized at the scale $\mu_{\rm F}$, so that the distribution amplitude depends on $\mu_{\rm F}$ as well. The insertion of the path-ordered gauge factor between the quark field operators in (6), which restores the gauge invariance of the non-local matrix element, is implied. The local limit of this operator corresponds to the conserved vector current, therefore

$$\int_0^1 \mathrm{d}z \, \phi_\parallel(z, \mu_{\rm F}) \tag{10}$$

is a renormalization-scale-invariant quantity and the normalization condition for the distribution amplitude

$$\int_0^1 \mathrm{d}z \, \phi_\parallel(z, \mu_{\rm F}) = 1 \tag{11}$$

corresponds to our convention for f_V. The kernel of the evolution equation (9) is known as an expansion in $\alpha_{\rm s}(\mu_{\rm F})$ up to the second order

$$V(z, z') \tag{12}$$

[1] Here and in the following we consider the *unprojected* impact factor, i.e. the impact factor as defined in (3) except for the singlet color projector $\delta^{cc'}/\sqrt{N_c^2 - 1}$. The application of the color projector on (5) will result in the replacement $\delta^{cc'} \to \sqrt{N_c^2 - 1}$.

$$= \frac{\alpha_s(\mu_F)}{2\pi} V^{(1)}(z,z') + \left(\frac{\alpha_s(\mu_F)}{2\pi}\right)^2 V^{(2)}(z,z') + \dots$$

For the purposes of the present work, we need to remind the expression for $V^{(1)}$,

$$V^{(1)}(z,z') = C_F \left[\frac{1-z}{1-z'}\left(1+\frac{1}{z-z'}\right)\theta(z-z') + \frac{z}{z'}\left(1+\frac{1}{z'-z}\right)\theta(z'-z)\right]_+ , \quad (13)$$

where

$$[f(z,z')]_+ \equiv f(z,z') - \delta(z-z')\int_0^1 \mathrm{d}t\, f(t,z) . \quad (14)$$

Let us now discuss briefly the cancellation of divergences in the final expression for the NLA impact factor. We perform the calculations with unrenormalized quantities, the bare strong coupling constant α_s and the bare meson distribution amplitude $\phi_\parallel^{(0)}(z)$. Therefore the NLA expression for the hard-scattering amplitude T_H expressed in terms of these quantities will contain both ultraviolet and infrared divergences, appearing as poles in the common dimensional regularization parameter ε. The ultraviolet divergences will disappear after the strong coupling constant renormalization. In the $\overline{\mathrm{MS}}$ scheme, it is given with the required accuracy by

$$\alpha_s = \alpha_s(\mu_R)\left[1 + \frac{\alpha_s(\mu_R)}{4\pi}\beta_0\left(\frac{1}{\hat\varepsilon} + \ln\left(\frac{\mu_R^2}{\mu^2}\right)\right)\right] , \quad (15)$$

where μ is the dimensional parameter introduced by the dimensional regularization,

$$\beta_0 = \frac{11\,N_c}{3} - \frac{2n_f}{3} , \quad \frac{1}{\hat\varepsilon} = \frac{1}{\varepsilon} + \gamma_E - \ln(4\pi) , \quad (16)$$

where n_f is the effective number of light quark flavors, γ_E is Euler's constant. The surviving infrared divergences will be only due to collinear singularities, the soft singularities cancel as usual after summing the "virtual" and the "real" parts of the radiative corrections. Since impact factors should be infrared-finite objects for physical transitions, it must be possible to absorb the remaining infrared divergences into the definition of the non-perturbative distribution amplitude. We will show that this is achieved by the substitution of the bare distribution amplitude by the renormalized one, given in the $\overline{\mathrm{MS}}$ scheme by

$$\phi_\parallel^{(0)}(z) \to \phi_\parallel(z,\mu_F) - \frac{\alpha_s(\mu_F)}{2\pi}\left(\frac{1}{\hat\varepsilon} + \ln\left(\frac{\mu_F^2}{\mu^2}\right)\right) \times \int_0^1 V^{(1)}(z,z')\phi_\parallel(z',\mu_F)\mathrm{d}z' , \quad (17)$$

which leads to a finite expression for T_H in the NLA. The success of the procedure described above and the finiteness of the z integral obtained in the factorization formula (5) would mean that the NLA impact factor in question can be unambiguously calculated in the collinear factorization approach.

3 Impact factor in LLA

Where the calculation of the impact factors in LLA is concerned, reggeons are equivalent to gluons with polarization vectors p_2^μ/s and the definition of the impact factor is reduced to the following integral of the κ-channel discontinuity of the reggeon (gluon) amplitude:

$$\Phi_{\gamma^*\to V} = -\mathrm{i}\int \frac{\mathrm{d}\kappa}{2\pi}\, \mathrm{Disc}_\kappa\, \mathcal{A}_{\gamma^* R\to V R'} , \quad (18)$$

where $\mathcal{A}_{\gamma^* R\to VR'}$ is given by the Fourier transform of the matrix element of the electromagnetic current $J^\mu_{\mathrm{em}} = -e_q\bar\Psi\gamma^\mu\,\Psi$,

$$(2\pi)^4\delta^4(p+q-p_1-q')\mathcal{A}_{\gamma^* R\to VR'} = \int \mathrm{d}^4x\,\mathrm{e}^{-\mathrm{i}(px)} e_\mu \langle V(p_1)R'|J^\mu_{\mathrm{em}}(x)|R\rangle , \quad (19)$$

e_μ being the polarization vector of the virtual photon.

The lowest order Feynman diagrams for $\mathcal{A}_{\gamma^* R\to VR'}$ having κ-channel discontinuity are shown in Fig. 2. Let us consider the diagram (a):

$$(2\pi)^4\delta^4(p+q-p_1-q')\mathcal{A}^{(a)}_{\gamma^* R\to VR'}$$

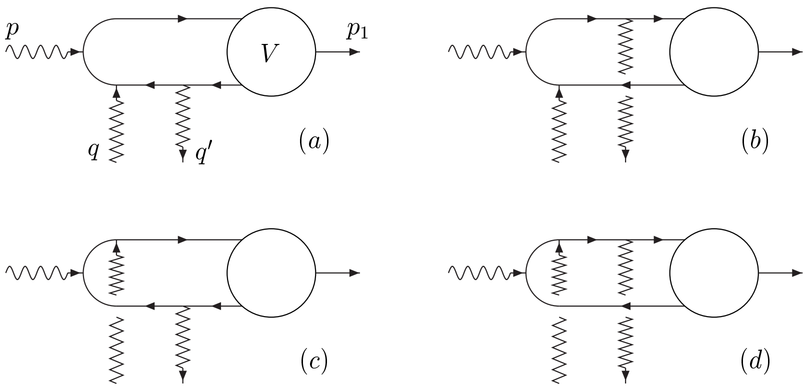

Fig. 2. Feynman diagrams at the lowest order for the $\gamma^* R \to VR'$ transition amplitude

$$= -e_q (\mathrm{i}g)^2 \int \mathrm{d}^4x \mathrm{d}^4y \mathrm{d}^4y_1 \mathrm{e}^{-\mathrm{i}(px)-\mathrm{i}(qy_1)+\mathrm{i}(q'y)}$$
$$\times \left(t^c t^{c'}\right)_{ij} e_\mu \langle V(p_1)|$$
$$\times T\left[\overline{\Psi}^i(x)\gamma^\mu \overbrace{\Psi(x)\overline{\Psi}(y_1)} \frac{\not p_2}{s} \overbrace{\Psi(y_1)\overline{\Psi}(y)} \frac{\not p_2}{s} \Psi^j(y)\right]$$
$$\times|0\rangle\,, \tag{20}$$

here the symbols $\overbrace{\Psi(x)\overline{\Psi}(y_1)}$ and $\overbrace{\Psi(y_1)\overline{\Psi}(y)}$ stand for the fermion propagators, g is the QCD coupling, $\alpha_\mathrm{s} = g^2/(4\pi)$, t^c and $t^{c'}$ denote the color generators in the fundamental representation and (i,j) are the quark color indices. Using translational invariance, color neutrality of the meson state and the Fierz identity, one can transform the meson matrix element to the form

$$\langle V(p_1)|\overline{\Psi}^i_\alpha(x)\Psi^j_\beta(y)|0\rangle$$
$$= \mathrm{e}^{\mathrm{i}(p_1y)}\langle V(p_1)|\overline{\Psi}^i_\alpha(x-y)\Psi^j_\beta(0)|0\rangle \tag{21}$$
$$= \mathrm{e}^{\mathrm{i}(p_1y)}\frac{\delta^{ij}}{N_c}\frac{1}{4}\left\{(\gamma^\mu)_{\beta\alpha}\langle V(p_1)|\overline{\Psi}(x-y)\gamma_\mu\Psi(0)|0\rangle + \dots\right\}\,,$$

where ellipsis stand for the contributions of other Fierz structures. Fierz projectors having an even number of γ matrices correspond to the chiral-odd configuration of the quark pair. Since in the massless limit chirality is conserved in the perturbative photon and gluon vertices, these chiral-odd structures do not contribute to the amplitude. Formally this appears as the vanishing of the trace of an odd number of γ matrices in the quark loop. For the chiral-conserving case there is another possibility beyond γ_μ, the Fierz structure $\gamma_\mu\gamma_5$. The light-cone expansion for this operator starts from twist-3 [21]; therefore it does not contribute to the impact factor at leading twist. The $\gamma_\mu\gamma_5$ operator is important for the production of transversely polarized vector mesons. It contributes, together with the twist-3 term parameterizing the γ_μ operator, to the leading power asymptotics for the transversely polarized meson impact factor. But, in comparison to the production of longitudinally polarized meson, the transverse case contains an additional suppression factor m_V/Q, therefore we will concentrate in what follows on the leading power asymptotics of the impact factor, which is given by the production of a longitudinally polarized meson.

Substituting (21) into (20) we obtain

$$\mathcal{A}^{(a)}_{\gamma^* R\to V_\mathrm{L} R'} = -\frac{e_q g^2 \delta^{cc'}}{8N_c}$$
$$\times\int \frac{\mathrm{d}^4l_1\mathrm{d}^4l_2\mathrm{d}^4(x-y)}{(2\pi)^4}\delta^4(l_1-l_2-q)\mathrm{e}^{-\mathrm{i}((p+l_1)(x-y))}$$
$$\times\mathrm{Sp}\left[\not e\frac{\not l_1}{l_1^2+\mathrm{i}\epsilon}\frac{\not p_2}{s}\frac{\not l_2}{l_2^2+\mathrm{i}\epsilon}\frac{\not p_2}{s}\gamma^\mu\right]$$
$$\times\langle V_\mathrm{L}(p_1)|\overline{\Psi}(x-y)\gamma_\mu\Psi(0)|0\rangle\,. \tag{22}$$

The leading power asymptotics of the integral (22) originates from the region where the interquark separation goes to the light-cone, $(x-y)^2\to 0$. Replacing the bilocal quark operator by its light-cone limit

$$\langle V_\mathrm{L}(p_1)|\overline{\Psi}(y)\gamma^\mu\Psi(0)|0\rangle_{y^2\to 0} = f_V p_1^\mu \int_0^1 \mathrm{d}z\, \mathrm{e}^{\mathrm{i}z(p_1y)}\phi_\parallel(z)\,, \tag{23}$$

and performing the integrals, we find

$$\mathcal{A}^{(a)}_{\gamma^* R\to V_\mathrm{L} R'}$$
$$= -\frac{e_q g^2 f_V \delta^{cc'}}{8N_c}\int_0^1 \mathrm{d}z\phi_\parallel(z)\int \mathrm{d}^4l_1\delta^4(p_1z-p-l_1)$$
$$\times\mathrm{Sp}\left[\not e\frac{\not l_1}{l_1^2+\mathrm{i}\epsilon}\frac{\not p_2}{s}\frac{\not l_1-\not q}{(l_1-q)^2+\mathrm{i}\epsilon}\frac{\not p_2}{s}\not p_1\right]\,. \tag{24}$$

This consideration shows that the quark lines entering the meson blob in Fig. 2a belong actually to the light-cone operator (23). The delta function in (24) means that the remaining part of the diagram which contributes to the hard-scattering amplitude is calculated for the quark and antiquark momenta, p_1z and $p_1\bar z$, being on-shell.

Going back from the reggeon scattering amplitude to the impact factor, we see that in LLA only one particle intermediate states contribute to the discontinuity in (18). In the case of the diagram Fig. 2a it is an antiquark cut

$$\frac{\mathrm{i}}{2\pi}\mathrm{Disc}_\kappa\frac{1}{(l_1-q)^2+\mathrm{i}\epsilon} \tag{25}$$
$$= \delta((l_1-q)^2) = \delta((p_1z-p-q)^2) = \delta(\bar z\kappa - z\mathbf{q}^2)\,.$$

According to (24) and (25), the contribution of diagram Fig. 2a to the impact factor reads

$$\Phi^{(a)}_{\gamma^*_\mathrm{L}\to V_\mathrm{L}} = -\frac{e_q g^2 f_V \delta^{cc'}(ep_1)}{2N_c Q^2}\int_0^1 \mathrm{d}z\,\phi_\parallel(z)\,. \tag{26}$$

We see that only the longitudinal polarization of the photon contributes. The polarization vector for longitudinally polarized photon reads

$$e_\mathrm{L} = \frac{1}{Q}p_1 + \frac{Q}{s}p_2 = \frac{1}{Q}p + 2\frac{Q}{s}p_2\,,\quad (e_\mathrm{L}p) = 0\,,\quad e_\mathrm{L}^2 = 1\,. \tag{27}$$

Due to the $U(1)$ gauge invariance, one can omit the first term in the above expression and use the simpler vector

$$e_\mathrm{L} \to e_\mathrm{L} = 2\frac{Q}{s}p_2\,. \tag{28}$$

The consideration of the other diagrams of Fig. 2 goes along similar lines. Here we cite the final result for the hard-scattering amplitude entering the LLA impact factor

$$T_\mathrm{H}^{(0)}(z,\alpha,s_0,\mu_\mathrm{F},\mu_\mathrm{R}) = \alpha_\mathrm{s}\frac{\alpha}{\alpha+z\bar z}\,. \tag{29}$$

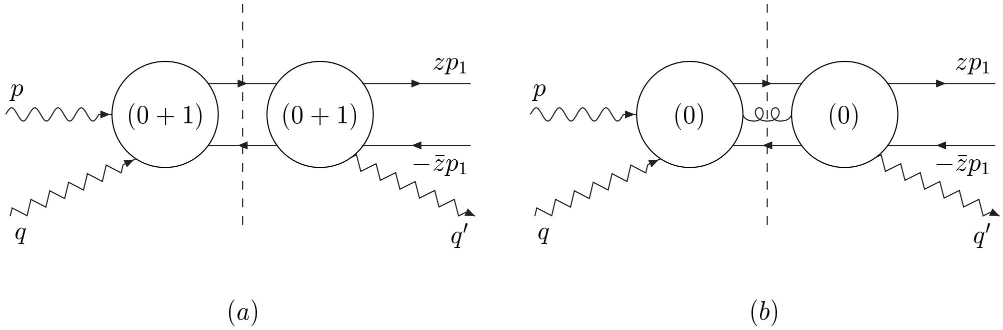

Fig. 3. The contributions to the impact factor from two-particle **a** and three-particle **b** intermediate states

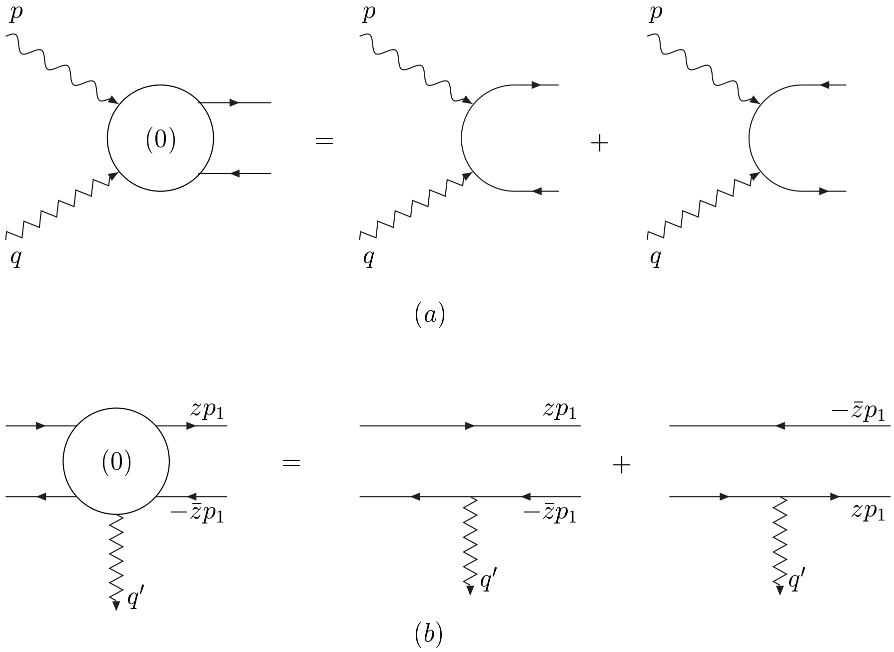

Fig. 4. The lowest order Feynman diagrams describing reggeon–photon **a** and reggeon–meson **b** vertices

This result coincides with what has been found in [22]. Note that the method used here may be directly applied to the calculation of the impact factors describing meson production at non-zero momentum transfer $\mathbf{\Delta}$ and for transverse polarization. Some results for the corresponding LLA impact factors may be found in [23, 24].

We see that due to collinear factorization, which effectively puts some fermion lines on the mass-shell, the complexity of the intermediate state contributing to the impact factor is reduced in comparison to the case of the virtual photon impact factor $\Phi_{\gamma^*\to\gamma^*}$. Actually we have a one-particle state instead of a two-particle one in the LLA, and as we will shortly see not more than two-particle intermediate states in the NLA, whereas a three-particle state contributes in the NLA to the $\Phi_{\gamma^*\to\gamma^*}$ impact factor. Due to this, the calculation of $\Phi_{\gamma^*\to V}$ is much simpler than that of $\Phi_{\gamma^*\to\gamma^*}$. This allows one to obtain closed analytical expression for the $\Phi_{\gamma^*\to V}$ impact factor in the NLA, as we show in the following section.

4 Impact factor in NLA

The impact factor is defined as an integral over the intermediate states produced in the γ^*–reggeon interaction, see (3). In the NLA both two-particle quark–antiquark $(q\bar{q})$ and three-particle quark–antiquark–gluon $(q\bar{q}g)$ intermediate states contribute. They are shown in Fig. 3a,b respectively. To calculate the impact factor in the NLA one has to know the $(q\bar{q})$ production vertices with NLA accuracy and the $(q\bar{q}g)$ ones at the Born level.

In the previous section we demonstrated in detail how the impact factor factorizes into a convolution of the distribution amplitude $\phi_\parallel(z)$ and the hard-scattering amplitude T_{H}, where the latter involves the $q\bar{q}$-pair production on the mass-shell. One can formulate a practical rule for the calculation of the meson impact factor. It can be obtained considering the impact factor describing the free $q\bar{q}$ production, $\Phi_{\gamma^*\to q\bar{q}}$, and replacing the quark spinors as follows:

$$v^i_\alpha(p_1\bar{z})\bar{u}^j_\beta(p_1 z) \to \frac{\delta^{ij}}{N_c}\frac{f_V}{4}\,(\not{p}_1)_{\alpha\beta}\,\phi_\parallel(z)\mathrm{d}z\,. \tag{30}$$

The Born reggeon–photon vertex is given by the two diagrams in Fig. 4a (see [22, 25])

$$\Gamma^{(0)}_{\gamma^*_{\mathrm{L}}q\bar{q}} = 2e_q g Q (t^c)_{ij} z\bar{z}\left(\frac{1}{\mathbf{q}_1^2+Q^2z\bar{z}} - \frac{1}{\mathbf{q}_2^2+Q^2z\bar{z}}\right)$$
$$\times \bar{u}^i_\alpha(q_1)\left(\frac{\not{p}_2}{s}\right)_{\alpha\beta} v^j_\beta(q_2)\,, \tag{31}$$

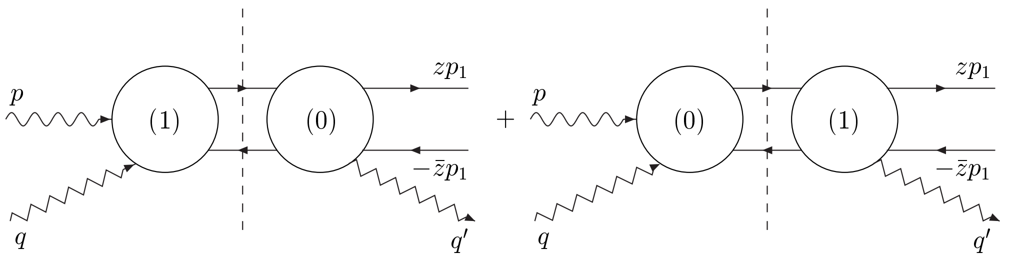

Fig. 5. The contribution of the quark–antiquark intermediate state at the next-to-leading order (NLO)

where q_1 and q_2 denote the momenta of the quark and of the antiquark. The contributions to the reggeon–meson vertex at the leading order are shown in Fig. 4b. Due to collinear factorization, quark lines labeled by $p_1 z$ and $p_1\bar{z}$ should be included in the definition of the meson distribution amplitude $\phi_\parallel(z)$. Therefore, for calculating $T_{\rm H}$ one can use the following expression for the LO reggeon–meson vertex:

$$\left(\Gamma^{(0)}_{V_{\rm L}q\bar{q}}\right)^* = \frac{gf_V}{4N_c}\,(t^{c'})_{ji}\,\phi_\parallel(z)\,{\rm d}z \tag{32}$$
$$\times\left[\bar{v}^j_\beta(q'+p_1\bar{z})\left(\frac{\not{p}_2}{s}\,\not{p}_1\right)_{\beta\alpha} + \left(\not{p}_1\frac{\not{p}_2}{s}\right)_{\beta\alpha} u^i_\alpha(p_1 z+q')\right],$$

where the first and the second terms represent the contributions of the first and the second diagrams of Fig. 4b, respectively. They have been drawn as disconnected diagrams, where the upper quark (antiquark) line is shown to indicate that, in the convolution of this vertex with the reggeon–photon one, the corresponding quark (antiquark) spinor in the expression of the reggeon–photon vertex (31) has to be amputated because this quark (antiquark) line is a part of $\phi_\parallel(z)$. Therefore the two-particle intermediate state $(q\bar{q})$ is effectively reduced to a one-particle antiquark (quark) state to be cut according to the definition of the impact factor. Performing the convolution of the two Born vertices given by (31) and (32) one gets again the result (29).

The radiation correction to the impact factor may be divided into two parts,

$$T^{(1)}_{\rm H} = T^{(q\bar{q})} + T^{(q\bar{q}g)}\,. \tag{33}$$

Here the first term represents the contribution of the $(q\bar{q})$ intermediate state shown in Fig. 5, when one of the reggeon effective vertices is taken at one-loop order. The second term in (33) is the $(q\bar{q}g)$ contribution, see Fig. 3b, which appears first only in the NLA. In that case, it is enough to take the corresponding reggeon interactions at the Born level. We proceed now to the evaluation of the $(q\bar{q})$ contribution.

4.1 Quark–antiquark intermediate state

According to Fig. 5, $T^{(q\bar{q})}$ is given by the sum of two terms which correspond to the corrections either to the reggeon–photon or to the reggeon–meson interaction:

$$T^{(q\bar{q})} = T^{(q\bar{q})}_{\gamma^*} + T^{(q\bar{q})}_V\,. \tag{34}$$

The NLA contribution to the reggeon–meson effective vertex is shown in Fig. 6 and it splits naturally into the sum of the three different contributions

$$T^{(q\bar{q})}_V = T^{(1\bar{q})}_V + T^{(1q)}_V + T^{(1{\rm c})}_V\,. \tag{35}$$

Here the first two terms represent the contributions of disconnected diagrams which are expressed in terms of NLA effective reggeon–antiquark and reggeon–quark vertices. They are similar to the disconnected diagrams of Fig. 4b which appear at the Born level. In the case of $T^{(1\bar{q})}_V$, the two-particle $(q\bar{q})$ intermediate state reduces effectively, due to collinear factorization, to a one-particle antiquark state, whereas in the case of $T^{(1q)}_V$ it reduces to a one-particle quark intermediate state. The last term in (35) stands for the contribution to $T^{(q\bar{q})}_V$ from the connected part of the NLA reggeon–meson effective vertex, which is shown in Fig. 7. The calculation of $T^{(1{\rm c})}_V$ involves the integration over the two-particle $(q\bar{q})$ state.

The virtual photon–reggeon effective vertices were studied in the NLA in [25]. Considering $T^{(q\bar{q})}_{\gamma^*}$, we found it convenient to distinguish two contributions denoted $T^{(1{\rm a})}_{\gamma^*}$ and $T^{(1{\rm b})}_{\gamma^*}$:

$$T^{(q\bar{q})}_{\gamma^*} = T^{(1{\rm a})}_{\gamma^*} + T^{(1{\rm b})}_{\gamma^*}\,. \tag{36}$$

According to Fig. 8, $T^{(1{\rm b})}_{\gamma^*}$ originates from the particular contribution to the photon–reggeon vertex given by the sum of two box diagrams shown in Fig. 8b; $T^{(1{\rm a})}_{\gamma^*}$ stands for the contribution to $T^{(q\bar{q})}_{\gamma^*}$ which comes from all other contributions to the NLA photon–reggeon vertex except those two box diagrams (for more details see [25]). The reason for such a separation is that we will combine and consider together the connected contribution to $T^{(q\bar{q})}_V$ and the contribution to $T^{(q\bar{q})}_{\gamma^*}$ coming from the box diagrams. This allows one to perform the cancellation of some terms in the sum of $T^{(1{\rm c})}_V$ and $T^{(1{\rm b})}_{\gamma^*}$ in intermediate steps of the calculation.

Thus, the contribution of the $(q\bar{q})$ intermediate state to the NLA impact factor may be represented as the sum of three terms:

$$T^{(q\bar{q})} = T_1 + T_2 + T_3\,, \tag{37}$$

where

$$T_1 = T^{(1{\rm a})}_{\gamma^*}\,,\quad T_2 = T^{(1{\rm c})}_V + T^{(1{\rm b})}_{\gamma^*}\,,\quad T_3 = T^{(1\bar{q})}_V + T^{(1q)}_V\,. \tag{38}$$

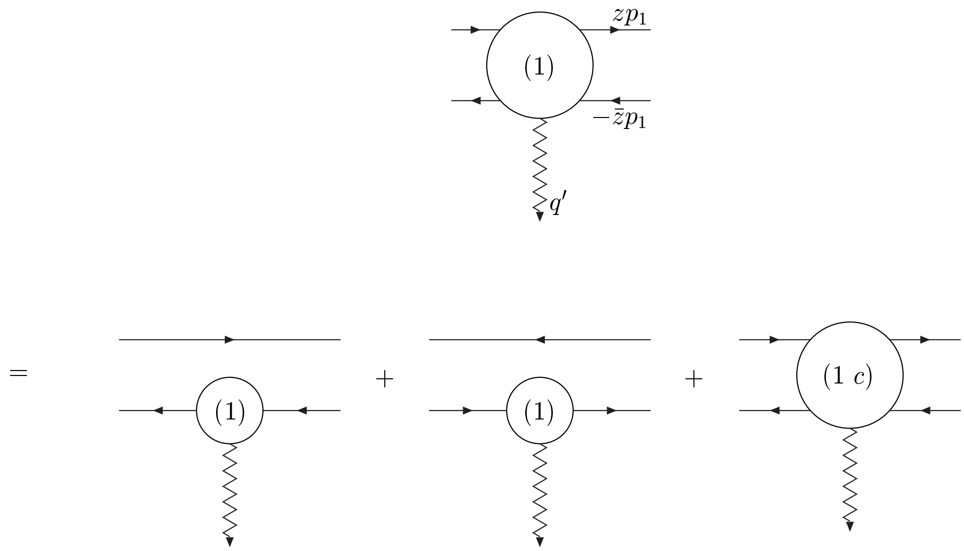

Fig. 6. The separation of the reggeon–meson NLO vertex into the connected (1c) and the disconnected (1) parts

Using the results of [25] and calculating the corresponding integrals in our kinematics, we find the following result for T_1:

$$T_1 = \frac{g^2 \Gamma[1-\varepsilon] \left(Q^2/\mu^2\right)^{\varepsilon}}{(4\pi)^{2+\varepsilon}} T_{\rm H}^{(0)} \left[\tau_1(z) + \tau_1(\bar{z}) \right] , \qquad (39)$$

where[2]

$$\begin{aligned}
\tau_1(z) &= -\frac{\beta_0}{4\varepsilon} + N_c \left[-\frac{1}{2\varepsilon^2} + \frac{3 - 2\ln\alpha - 4\ln z}{4\varepsilon} \right] \\
&+ \frac{1}{N_c \varepsilon} \left[-\frac{1}{4} + \frac{\alpha + z\bar{z}}{2\,(\alpha - z^2)} - \frac{\alpha\,(z + \alpha\bar{z})}{\alpha^2 - z^2} \right. \\
&- \frac{z^2}{2\,(\alpha - z^2)^2} \ln\alpha + \frac{\alpha(\alpha + z\bar{z})}{2(\alpha - z)^2} \ln\left(\frac{\alpha}{z}\right) \\
&\left. + \left(\frac{\alpha\, z^3}{2\,\bar{z}(\alpha + z)^2} - \frac{z^2}{2(\alpha - z^2)^2} \right) \ln\left(\frac{\alpha + z\bar{z}}{\alpha z}\right) \right] \\
&+ n_f \left[-\frac{5}{18} + \frac{\ln\alpha}{6} \right] \\
&+ \frac{1}{N_c} \left[1 - \frac{5\,z}{4\,(\alpha - z^2)} + \frac{5\,z\,(\alpha + z\bar{z})}{2\,(\alpha^2 - z^2)} \right. \\
&- \left(\frac{2 - z}{4\bar{z}} + \frac{(2 - z)\,z}{2\,(\alpha - z)} \right. \\
&\left. + \frac{5\,z^4}{4\,\bar{z}\,(\alpha + z)^2} - \frac{z^2\,(2 + 3\,z)}{4\,\bar{z}\,(\alpha + z)} \right) \ln\alpha \\
&+ \frac{1 - 2z\bar{z}}{8\alpha} \ln\left(\frac{\alpha + z\bar{z}}{z\bar{z}}\right) \\
&+ \left(\frac{\alpha\,(\alpha + z\bar{z})}{4\,(\alpha - z)^2} - \frac{\alpha\, z^3}{4\,\bar{z}\,(\alpha + z)^2} \right) \ln^2\alpha \\
&- \frac{\alpha(\alpha + z\bar{z})}{4(\alpha - z)^2} \ln^2 z \\
&+ \left(\frac{1 - 2\,z}{4\,\bar{z}} + \frac{7\,z - z^2}{4\,(\alpha - z)} + \frac{5\,\left(2\,z^2 - z^3\right)}{4\,(\alpha - z)^2} \right) \ln\left(\frac{z}{\alpha}\right) \\
&+ \left(\frac{5\,z^4}{4\,\bar{z}\,(\alpha + z)^2} - \frac{4\,z^2 + z^3}{4\,\bar{z}\,(\alpha + z)} \right. \\
&\left. + \frac{6\,z^2 - 4\,z^3 - \alpha + 4\,z\,\alpha}{4\,(\alpha - z^2)^2} \right) \ln\left(\frac{\alpha + z\bar{z}}{z}\right) \\
&\left. + \left(\frac{\alpha\, z^3}{4\,\bar{z}\,(\alpha + z)^2} - \frac{z^2}{4\,(\alpha - z^2)^2} \right) \ln^2\left(\frac{\alpha + z\bar{z}}{z}\right) \right] \\
&+ N_c \left[\frac{1}{9} + \frac{\alpha(\alpha + z\bar{z})}{4\,(\alpha - z)\,(\alpha - z^2)} \right. \\
&- \frac{3}{4} \ln^2\alpha - \frac{1}{2} \ln^2\left(\frac{\alpha + z\bar{z}}{z}\right) \\
&+ \left(\frac{z^3}{4\,\bar{z}\,(\alpha - z^2)^2} + \frac{z}{2\,(\alpha - z^2)} - \frac{z^2}{4\,\bar{z}\,(\alpha + z)} \right) \\
&\times \ln\left(\frac{\alpha + z\bar{z}}{z}\right) \\
&- \left(\frac{1}{6} + \frac{\alpha + z\bar{z}}{4\bar{z}\,(\alpha + z)} \right) \ln\alpha \\
&+ \frac{\alpha^2 - 2\,\bar{z}\,z^2 - \alpha\,z(1 + z)}{4\,\bar{z}\,(\alpha - z)^2} \ln\left(\frac{\alpha}{z}\right) \\
&- \ln\left(\frac{\alpha + z}{z^2}\right) \ln\left(\frac{\alpha + z\bar{z}}{\alpha z}\right) \\
&- \mathrm{Li}_2\left(-\frac{z}{\alpha}\right) + \mathrm{Li}_2\left(-\frac{z\bar{z}}{\alpha}\right) - \mathrm{Li}_2\left(z - \frac{\alpha}{z}\right)
\end{aligned}$$

[2] Here and in the expressions for $\tau_2(z), \ldots, \tau_5(z)$ which will appear below we used the $z \leftrightarrow \bar{z}$ symmetry in order to simplify the results.

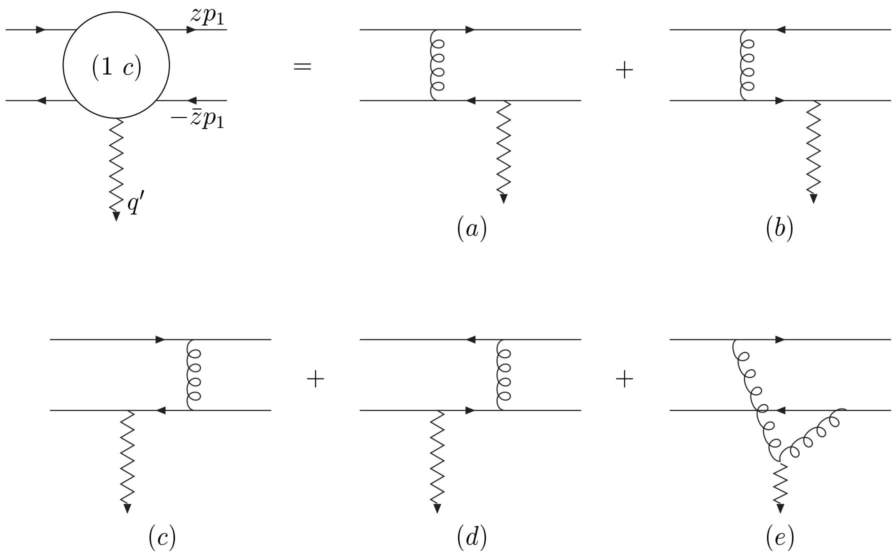

Fig. 7. The Feynman diagrams for the connected reggeon–meson vertex

$$- \mathrm{Li}_2\left(-\frac{\alpha+z\bar{z}}{z^2}\right)\Bigg] \tag{40}$$

and

$$\mathrm{Li}_2(z) = -\int\limits_0^z \frac{\mathrm{d}t}{t}\ln(1-t)\ . \tag{41}$$

Our result for T_2 is

$$T_2 = \frac{g^2\Gamma[1-\varepsilon]\left(Q^2/\mu^2\right)^{\varepsilon}}{(4\pi)^{2+\varepsilon}}T_{\mathrm{H}}^{(0)}\left[\tau_2(z)+\tau_2(\bar{z})\right]\ , \tag{42}$$

where

$$\begin{aligned}
\tau_2(z) &= \frac{\alpha+z\bar{z}}{\alpha}\int\frac{\mathrm{d}^{2+2\varepsilon}\mathbf{l}\left(Q^2\right)^{1-\varepsilon}}{\pi^{1+\varepsilon}\Gamma[1-\varepsilon]}\int\limits_0^1\mathrm{d}u\,\frac{u\bar{u}}{z\bar{z}}\\
&\times\Bigg[\left(\frac{1-\varepsilon}{4}C_{\mathrm{F}}+\frac{1}{4N_c}\right)\left(\frac{1}{(\mathbf{l}-\mathbf{q})^2}-\frac{1}{\mathbf{l}^2}\right)\frac{1}{\mathbf{l}^2+Q^2u\bar{u}}\\
&-\frac{1}{2N_c}\Bigg(\bar{z}(u-z)\\
&\times\frac{(1+\varepsilon)\bar{z}\mathbf{l}^2-(1+(1+\varepsilon)(u-z))\,(\mathbf{l}\mathbf{q})+u\mathbf{q}^2}{\mathbf{l}^2\left[(\mathbf{l}-\mathbf{q})^2+Q^2u\bar{u}\right](\mathbf{l}\bar{z}-(u-z)\mathbf{q})^2}\\
&+\frac{\bar{u}z^3\bar{z}^2\left[(1+\varepsilon)\bar{z}\mathbf{l}^2-(1-(1+\varepsilon)z\bar{u})\,(\mathbf{l}\mathbf{q})+uz\mathbf{q}^2\right]}{\mathbf{l}^2\left[\bar{z}\,(\mathbf{l}-\bar{u}\mathbf{q})^2+u\bar{u}\left(\mathbf{q}^2+Q^2z\bar{z}\right)\right](\mathbf{l}\bar{z}+z\bar{u}\mathbf{q})^2}\\
&-uz^2\\
&\times\frac{(1+\varepsilon)z\mathbf{l}^2-(1+(1+\varepsilon)zu)\,(\mathbf{l}\mathbf{q})+(1-\bar{u}z)\mathbf{q}^2}{\mathbf{l}^2\left[\mathbf{l}^2+Q^2u\bar{u}z\right](\mathbf{l}-u\mathbf{q})^2}\Bigg)\Bigg]\ .
\end{aligned} \tag{43}$$

Note that the box diagrams in Fig. 8b and the diagrams Fig. 7a,b contain imaginary parts. But combined together in T_2 these imaginary parts cancel. We made this cancellation explicit proceeding in the following way. In the loop integrals for box diagrams we split the loop integration into the integral over the transverse part of the loop momentum and the integral over the two Sudakov variables. Then, we performed the integration over one of the Sudakov variables. After that, we combined the results for box diagrams with all other contributions to T_2 and using some algebraic transformations obtained the representation (43).

The integration of (43) gives

$$\begin{aligned}
\tau_2(z) &= \frac{C_{\mathrm{F}}}{\varepsilon}\left[-\frac{\alpha+z\bar{z}}{4\,c\,z\bar{z}}\,\ln\left(\frac{2\,c+1}{2\,c-1}\right)\right]\\
&+\frac{1}{N_c}\Bigg[\frac{1}{2\,\varepsilon^2}+\frac{1}{\varepsilon}\Bigg(\frac{z\,(\alpha+z\bar{z})}{\alpha^2-z^2}\\
&-\frac{\alpha+z\bar{z}}{2\,(\alpha-z^2)}+\left(\frac{1}{2}+\frac{z^2}{2\,(\alpha-z^2)^2}\right)\ln\alpha\\
&+\frac{\alpha\,(\alpha+z\bar{z})}{2\,(\alpha-z)^2}\ln\left(\frac{z}{\alpha}\right)\\
&+\left(\frac{z^2}{2\,(\alpha-z^2)^2}-\frac{\alpha z^3}{2\bar{z}\,(\alpha+z)^2}\right)\ln\left(\frac{\alpha+z\bar{z}}{\alpha z}\right)\Bigg)\Bigg]\\
&+C_{\mathrm{F}}\Bigg[\frac{\alpha+z\bar{z}}{2z\bar{z}}\Bigg(\frac{1}{\alpha}\left(2\,c\,\ln\left(\frac{2\,c+1}{2\,c-1}\right)+\ln\alpha\right)\\
&+\frac{1}{c}\Bigg(\frac{\pi^2}{6}+\ln\alpha\ln4-\ln^2c\\
&+2\ln c\ln\left(\frac{2\,c-1}{4}\right)-\ln^2(2\,c+1)+\frac{1}{2}\ln\left(\frac{2\,c+1}{2\,c-1}\right)\\
&+\frac{1}{4}\ln^2\left(\frac{2\,c+1}{2\,c-1}\right)-2\mathrm{Li}_2\left(\frac{2\,c-1}{4\,c}\right)\\
&-\mathrm{Li}_2\left(\frac{2}{1+2\,c}\right)\Bigg)\Bigg)\Bigg]\\
&+\frac{1}{N_c}\left[\frac{\alpha+z\bar{z}}{4z^2\bar{z}^2}\left(2\,c\,\ln\left(\frac{2\,c+1}{2\,c-1}\right)+\ln\alpha-2\right)\right.
\end{aligned}$$

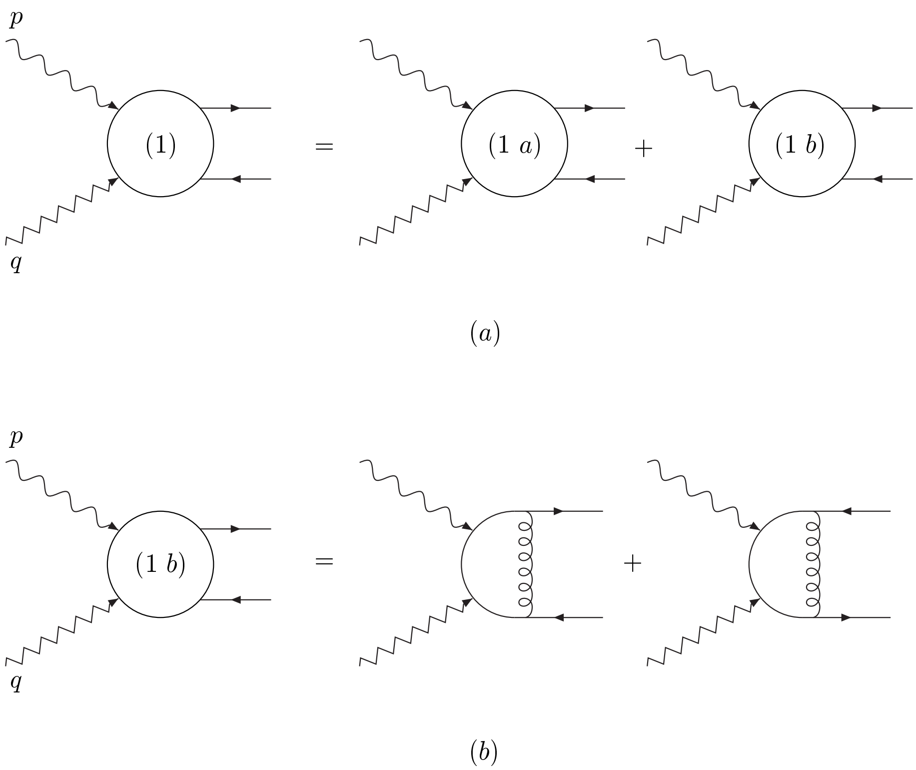

Fig. 8. a The separation of the NLO virtual photon–reggeon vertex into the sum of two contributions (1a) and (1b). **b** The contribution (1b) is given by two box diagrams

$$
-\frac{\alpha^2+\alpha z-\bar z z^3}{2z^3\bar z}\left(\ln\left(\frac{\alpha z}{\alpha+z\bar z}\right)\ln\left(\frac{\alpha+z}{\alpha}\right)\right.
$$
$$
+\ln\left(\frac{2c+1}{2c-1}\right)\ln\left(\frac{2\alpha+z(1+2c)}{2\alpha+z(1-2c)}\right)
$$
$$
+\frac{\pi^2}{6}+2\mathrm{Li}_2\left(\frac{2z}{1-2c}\right)+2\mathrm{Li}_2\left(\frac{2z}{1+2c}\right)-\mathrm{Li}_2\left(-\frac{z}{\alpha}\right)
$$
$$
+\mathrm{Li}_2\left(-\frac{z^2}{\alpha+z\bar z}\right)
$$
$$
\left.+\mathrm{Li}_2\left(z-\frac{\alpha}{z}\right)+\frac{1}{2}\ln^2\left(\frac{\alpha+z\bar z}{\alpha}\right)\right)
$$
$$
-\frac{\pi^2}{12}+\frac{3+2z}{2z}+\frac{\alpha}{2z^2\bar z^2}-\frac{8z-9z^2}{4\bar z(\alpha-z)}
$$
$$
+\frac{5z-4z^2}{4\bar z(\alpha-z^2)}+\frac{5z^3}{2(\alpha^2-z^2)}
$$
$$
+\left(\frac{5z^4}{4\bar z(\alpha+z)^2}+\frac{3z-z^2-\alpha}{2(\alpha-z)}-\frac{3z^2+3z^3}{4\bar z(\alpha+z)}\right)\ln\alpha
$$
$$
+\left(\frac{1}{4}+\frac{\alpha z^3}{4\bar z(\alpha+z)^2}\right)\ln^2\alpha+\frac{1-2z\bar z}{8\alpha}\ln\left(\frac{z\bar z}{\alpha+z\bar z}\right)
$$
$$
+\frac{1}{4z\bar z}\ln(\alpha+z\bar z)
$$
$$
+\left(\frac{1}{4}+\frac{3z-z^2}{4(\alpha-z)}+\frac{2z^2-z^3}{4(\alpha-z)^2}\right)\left(\ln^2 z-\ln^2\alpha\right)
$$
$$
-\left(\frac{1}{2}+\frac{4z-7z^2+z^3}{4\bar z(\alpha-z)}+\frac{8z^2-14z^3+5z^4}{4\bar z(\alpha-z)^2}\right)
$$
$$
\times\ln\left(\frac{z}{\alpha}\right)
$$
$$
+\left(\frac{5z^2+z^3}{4\bar z(\alpha+z)}-\frac{5z^4}{4\bar z(\alpha+z)^2}-\frac{5z^2-4z^3}{4\bar z(\alpha-z^2)^2}\right.
$$
$$
\left.+\frac{1-5z+6z^2}{4\bar z(\alpha-z^2)}\right)\ln\left(\frac{\alpha+z\bar z}{z}\right)
$$
$$
+\left(\frac{1}{4}-\frac{\alpha z^3}{4\bar z(\alpha+z)^2}-\frac{\alpha(\alpha+z)}{4\bar z z^3}+\frac{z^2}{4(\alpha-z^2)^2}\right)
$$
$$
\left.\times\ln^2\left(\frac{\alpha+z\bar z}{z}\right)\right], \qquad (44)
$$

where we used the notation $c=\sqrt{\alpha+1/4}$.

Finally, using the result for the NLA quark–quark–reggeon effective vertex [26] we obtain

$$
T_3=\frac{g^2\Gamma[1-\varepsilon]\left(Q^2/\mu^2\right)^\varepsilon}{(4\pi)^{2+\varepsilon}}T_{\mathrm{H}}^{(0)}\left[\tau_3(z)+\tau_3(\bar z)\right], \qquad (45)
$$

where

$$
\tau_3(z)=-\frac{\beta_0}{4\varepsilon}
$$
$$
+C_{\mathrm{F}}\left[-\frac{1}{\varepsilon^2}+\frac{3}{2\varepsilon}-\frac{\ln\alpha+2\ln z}{\varepsilon}\right]-\frac{\ln z}{N_c\varepsilon}
$$
$$
+n_f\left[-\frac{5}{18}+\frac{\ln\alpha}{6}\right]
$$

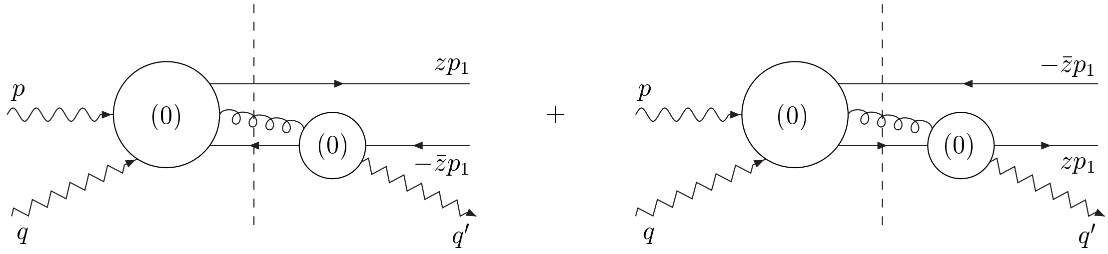

(a)

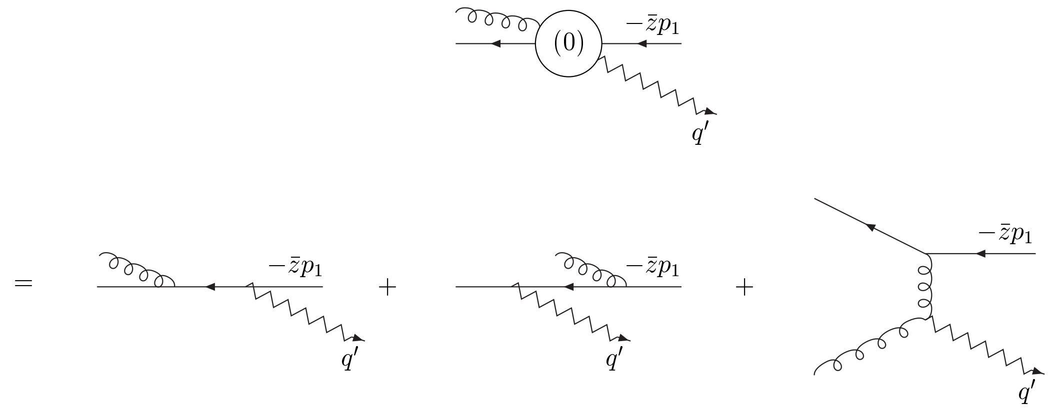

(b)

Fig. 9. a The separation of the $(q\bar{q}g)$ contribution to the impact factor into the sum of the antiquark–gluon and the quark–gluon cuts. **b** The lowest order Feynman diagrams for the gluon bremsstrahlung vertex

$$+C_{\mathrm{F}}\left[\frac{13}{18}+\frac{2\pi^2}{3}-\frac{\ln\alpha}{3}-\frac{1}{2}\ln^2\alpha-2\ln\alpha\ln z\right]$$
$$+\frac{1}{N_c}\left[\frac{85+9\pi^2}{36}-\frac{11\ln\alpha}{12}-\ln\alpha\ln z\right]. \qquad (46)$$

4.2 Quark–antiquark–gluon intermediate state

We proceed now to the evaluation of the contribution to the impact factor from the $(q\bar{q}g)$ intermediate state shown in Fig. 3b. For this purpose we need the $(q\bar{q}g)$ production vertices at the Born level. Examining the Feynman diagrams for the corresponding reggeon–meson vertex, one can easily see that at the Born level only disconnected diagrams contribute, i.e. in each diagram either the quark or the antiquark cut line enters directly the meson vertex and therefore is absorbed into the definition of the meson distribution amplitude. Thus the reggeon–meson vertex can be represented as the sum of two contributions,

$$\Gamma_{V_{\mathrm{L}}q\bar{q}g}=\Gamma^{q}_{V_{\mathrm{L}}q\bar{q}g}+\Gamma^{\bar{q}}_{V_{\mathrm{L}}q\bar{q}g}\,. \qquad (47)$$

Consequently, one deals here with the contributions of effective two-particle intermediate states, the antiquark–gluon one (related to $\Gamma^{q}_{V_{\mathrm{L}}q\bar{q}g}$) and the quark–gluon one (related to $\Gamma^{\bar{q}}_{V_{\mathrm{L}}q\bar{q}g}$), which are shown in the first and the second diagrams in Fig. 9a. Since due to the charge conjugation symmetry these two contributions are related to each other, it is enough to evaluate one of them, say the first diagram of Fig. 9a, with the effective antiquark–gluon cut. The result for the diagram with the effective quark–gluon cut is obtained from the contribution of the antiquark–gluon one by the replacement $z\to\bar{z}$. Therefore, in what follows we will consider the antiquark–gluon cut.

According to the first diagram in Fig. 9a, to calculate $\Gamma^{q}_{V_{\mathrm{L}}q\bar{q}g}$ one needs to consider the gluon bremsstrahlung from the antiquark line, described by the three diagrams shown in Fig. 9b. After a simple calculation we obtain the following result for the corresponding part of the reggeon–meson vertex

$$\left(\Gamma^{q}_{V_{\mathrm{L}}q\bar{q}g}\right)^{*}=-\frac{g^2 f_V}{4N_c} \qquad (48)$$
$$\times\bar{v}^{j}_{\beta}(q_2)\left(\left[2\bar{z}\,(\mathbf{T}e^{\,a})+z_3\,\not{e}^{\,a}_{\perp}\not{T}\right]\frac{\not{p}_2}{s}\,\not{p}_1\right)_{\beta\alpha}\phi_{\|}(z)\,\mathrm{d}z\,.$$

Here $q_2=z_2p_1+(\mathbf{q}_2^2/z_2)(p_2/s)+q_{2\perp}$ denotes the momentum of the cut antiquark, the momentum of the cut gluon is $k=z_3p_1+(\mathbf{k}^2/z_3)(p_2/s)+k_\perp$,

$$z_2+z_3=1-z\,,\qquad k_\perp+q_{2\perp}=q_\perp\,. \qquad (49)$$

The polarization state of the cut gluon is described by the 4-vector e^a, which can be expressed in the gauge $e^ap_2=0$

as

$$e^a = \frac{2(\mathbf{e}^{\,a}\mathbf{k})}{z_3\, s} p_2 + e^a_\perp\,, \quad e^a k = 0\,, \tag{50}$$

where the index a describes the color state of the gluon, and the transverse vector $e^a_\perp$ parameterizes two different physical polarization states of the gluon, $(e_\perp^{\,a})^2 = -(\mathbf{e}^{\,a})^2$. The other transverse vector entering (48) is

$$\mathbf{T} = \left(\frac{\bar z \mathbf{q}_2 - z_2\mathbf{q}}{(\bar z\mathbf{q}_2 - z_2\mathbf{q}\,)^2} - \frac{\mathbf{q}_2}{\bar z \mathbf{q}_2^2}\right)(t^a t^{c'})_{ji} + \frac{1}{\bar z}\left(\frac{\mathbf{k}}{\mathbf{k}^2} + \frac{\mathbf{q}_2}{\mathbf{q}_2^2}\right)(t^{c'}t^a)_{ji}\,, \tag{51}$$

where the indices i, j describe the color states of the quark and of the antiquark, respectively.

The reggeon–photon ($q\bar q g$) production vertex was considered in [25]. Similarly to the reggeon–meson vertex discussed above, we rewrite the reggeon–photon vertex in terms of the transverse gluon polarization vector $e^a_\perp$ and of the other two transverse vectors which we denote $\mathbf{T}_q$ and $\mathbf{T}_{\bar q}$:

$$\Gamma_{\gamma^*_{\rm L} q\bar q g} = -2\, e_q\, g^2\, Q\, \bar u^i_\alpha(z p_1) \times \left([2\,(\mathbf{e}^{\,a}(\mathbf{T}_q \bar z - \mathbf{T}_{\bar q} z)) + z_3\,(\not{T}_q + \not{T}_{\bar q})\not{e}^a_\perp]\,\frac{\not{p}_2}{s}\right)_{\alpha\beta} \times v^j_\beta(q_2)\,, \tag{52}$$

where

$$\mathbf{T}_q = \left(\frac{\bar z\mathbf{q}_2 - z_2\mathbf{q}}{(\bar z\mathbf{q}_2 - z_2\mathbf{q})^2}\left(\frac{1}{Q^2} - \frac{1}{Q^2 + \frac{\mathbf{q}^{\,2}}{z} + \frac{\mathbf{q}_2^2}{z_2} + \frac{\mathbf{k}^2}{z_3}}\right) - \frac{\mathbf{q}_2}{Q^2 + \frac{\mathbf{q}_2^2 \bar z}{z_2 z_3}}\frac{1}{Q^2 z_2 z_3}\right)(t^c t^a)_{ij} + \frac{1}{Q^2 z_2 z_3}\left(\frac{\mathbf{k}}{Q^2 + \frac{\mathbf{k}^2\bar z}{z_2 z_3}} + \frac{\mathbf{q}_2}{Q^2 + \frac{\mathbf{q}_2^2 \bar z}{z_2 z_3}}\right)(t^a t^c)_{ij}\,, \tag{53}$$

and

$$\mathbf{T}_{\bar q} = (t^c t^a)_{ij} \times \left(\frac{z\mathbf{q}_2 - \bar z_2\mathbf{q}}{(z\mathbf{q}_2 - \bar z_2\mathbf{q})^2}\left(\frac{1}{Q^2 + \frac{\mathbf{q}_2^2}{z_2\bar z_2}} - \frac{1}{Q^2 + \frac{\mathbf{q}^{\,2}}{z} + \frac{\mathbf{q}_2^2}{z_2} + \frac{\mathbf{k}^2}{z_3}}\right) + \frac{\mathbf{q}_2}{Q^2 + \frac{\mathbf{q}_2^2}{z_2\bar z_2}}\frac{1}{Q^2 z z_2 \bar z_2} - \frac{\mathbf{q}_2}{Q^2 + \frac{\mathbf{q}_2^2\bar z}{z_2 z_3}}\frac{\bar z}{Q^2 z z_2 z_3}\right) + \frac{(t^a t^c)_{ij}}{z}\left(\frac{\mathbf{k}}{\mathbf{k}^2}\left(\frac{1}{Q^2 + \frac{\mathbf{q}_2^2}{z_2\bar z_2}} - \frac{1}{Q^2}\right) + \frac{\bar z}{Q^2 z_2 z_3}\left(\frac{\mathbf{k}}{Q^2 + \frac{\mathbf{k}^2\bar z}{z_2 z_3}} + \frac{\mathbf{q}_2}{Q^2 + \frac{\mathbf{q}_2^2\bar z}{z_2 z_3}}\right) - \frac{\mathbf{q}_2}{Q^2 + \frac{\mathbf{q}_2^2}{z_2\bar z_2}}\frac{1}{Q^2 z_2 \bar z_2}\right)\,, \tag{54}$$

with $\bar z_2 = 1 - z_2 = z + z_3$.

Note that the quantities $\mathbf{T}$, $\mathbf{T}_q$ and $\mathbf{T}_{\bar q}$ and, therefore, the reggeon vertices $\Gamma_{V_{\rm L} q\bar q g}$ and $\Gamma_{\gamma^*_{\rm L} q\bar q g}$, vanish when the reggeon transverse momentum $\mathbf{q}$ tends to zero.

The convolution[3] of the reggeon vertices (52) and (48), with the subsequent summation over the Dirac and the color indices of the cut antiquark and gluon, gives the following contribution of the diagrams in Fig. 9a to the impact factor:

$$-\frac{e_q g^4 f_V Q}{N_c (2\pi)^{3+2\varepsilon}} \int\limits_0^1 \phi_\parallel(z)\,{\rm d}z \int\limits_0^{\bar z} \frac{{\rm d}z_3}{z_3}\,{\rm d}^{2+2\varepsilon}\mathbf{q}_2\,\theta(s_\Lambda - \kappa) \times \left[(\mathbf{T}_q\mathbf{T})(2\bar z z_2 + (1+\varepsilon)z_3^2) + (\mathbf{T}_{\bar q}\mathbf{T})(z_3(2z-1) - 2z\bar z + (1+\varepsilon)z_3^2)\right]\,, \tag{55}$$

where in $(\mathbf{T}_q\mathbf{T})$ and $(\mathbf{T}_{\bar q}\mathbf{T})$ the sum over the quark and the gluon color indices i, j and a is implied. The integrals over ${\rm d}z_3$ and ${\rm d}^{2+2\varepsilon}\mathbf{q}_2$ in (55) stand for the integration over the antiquark–gluon intermediate state. For $z_3 \to 0$ the integral (55) would diverge if the invariant mass κ were allowed to become arbitrarily large, this corresponding to the radiation of the gluon in the central region, away from the fragmentation region of the virtual photon. Such a gluon radiation has to be assigned to the reggeon Green's function and subtracted from the impact factor. The corresponding separation procedure, described in [3,17], leads to the appearance of the $\theta(s_\Lambda - \kappa)$ in the definition of the impact factor (see (3)) and to the need to subtract the so-called counterterm, given by the second term in the RHS of (3). Since

$$\kappa = \frac{\mathbf{k}^2}{z_3} + \frac{\mathbf{q}_2^{\,2}}{z_2} - \mathbf{q}^{\,2} \tag{56}$$

and the integral is restricted by the condition $\theta(s_\Lambda - \kappa)$, with $s_\Lambda \to \infty$, the lower boundary of the z_3 integral in (55) is $z_3^{\rm min} = \frac{\mathbf{k}^2}{s_\Lambda}$.

We define the divergent part of (55) for $z_3 \to 0$ as

$$-\frac{2e_q g^4 f_V Q}{N_c(2\pi)^{3+2\varepsilon}} \times \int\limits_0^1 \phi_\parallel(z)\,{\rm d}z \int\limits_0^{\bar z} \frac{{\rm d}z_3}{z_3}{\rm d}^{2+2\varepsilon}\mathbf{q}_2\,[\bar z(\mathbf{T}_q\bar z - \mathbf{T}_{\bar q}z)\mathbf{T}]_{z_3\to 0}\,, \tag{57}$$

where

$$[\bar z(\mathbf{T}_q\bar z - \mathbf{T}_{\bar q}z)\mathbf{T}]_{z_3\to 0} = \frac{N_c\delta^{cc'}}{2Q^2}\frac{\mathbf{q}^{\,2}}{\mathbf{k}^2[\mathbf{q}_2^{\,2} + Q^2 z\bar z]}\,. \tag{58}$$

[3] Beforehand, the quark spinor $\bar u^i_\beta(p_1 z)$ has to be amputated from the photon vertex, since it belongs to the definition of the meson distribution amplitude.

Integrating over z_3 in (57) we obtain

$$-\frac{e_q g^4 f_V \delta^{cc'}}{Q(2\pi)^{3+2\varepsilon}} \times \int_0^1 \phi_\parallel(z)\,\mathrm{d}z \int \mathrm{d}^{2+2\varepsilon}\mathbf{q}_2 \frac{\mathbf{q}^{\,2}}{(\mathbf{q}_2-\mathbf{q})^2[\mathbf{q}_2^{\,2}+Q^2 z\bar{z}]} \times \ln\left(\frac{\bar{z}s_\Lambda}{(\mathbf{q}_2-\mathbf{q})^2}\right) . \tag{59}$$

The consideration of the contribution of the quark-gluon cut diagrams shown on the right picture in Fig. 9a goes along the same lines. Similarly to (59), we define the contribution which is singular for $s_\Lambda \to \infty$, given by the replacement $z \to \bar{z}$ in (59). Then in the sum of these two contributions with the BFKL subtraction term we find that s_Λ cancels out and arrive at some finite contribution to the impact factor which is denoted below as T_4. Thus, the total contribution of the $(q\bar{q}g)$ intermediate state to the NLA impact factor may be represented as the sum of two terms,

$$T^{(q\bar{q}g)} = T_4 + T_5\,, \tag{60}$$

where the results for T_4 and T_5 are presented, as usual, in the form

$$T_{4,5} = \frac{g^2\Gamma[1-\varepsilon]\left(Q^2/\mu^2\right)^\varepsilon}{(4\pi)^{2+\varepsilon}} T_{\mathrm{H}}^{(0)}\left[\tau_{4,5}(z)+\tau_{4,5}(\bar{z})\right] . \tag{61}$$

The procedure described above gives for τ_4 the following expression:

$$\tau_4(z) = \frac{(\alpha+z\bar{z})N_c\left(Q^2\right)^{1-\varepsilon}}{\pi^{1+\varepsilon}\Gamma[1-\varepsilon]} \times \int \frac{d^{2+2\varepsilon}\mathbf{q}_2}{(\mathbf{q}_2-\mathbf{q})^2[\mathbf{q}_2^{\,2}+Q^2 z\bar{z}]}\ln\left(\frac{z\bar{z}s_0}{(\mathbf{q}_2-\mathbf{q})^2}\right) + \frac{N_c\,\Gamma^2[1+\varepsilon](\alpha)^\varepsilon}{\varepsilon\,\Gamma[1+2\varepsilon]}\ln\left(\frac{\alpha Q^2}{s_0}\right) , \tag{62}$$

and for $\tau_5(z)$ one arrives naturally at two contributions:

$$\tau_5(z) = \tau_5^a(z) + \tau_5^b(z)\,, \tag{63}$$

where

$$\delta^{cc'}\,\tau_5^a(z) = \frac{2\left(Q^2\right)^{1-\varepsilon}}{\pi^{1+\varepsilon}\Gamma[1-\varepsilon]}\frac{(\alpha+z\bar{z})}{\alpha} \times \int_0^{\bar{z}} \frac{\mathrm{d}z_3}{z_3}\mathrm{d}^{2+2\varepsilon}\mathbf{q}_2 \times \left[2\bar{z}^2\left(\mathbf{T}_q\mathbf{T} - \mathbf{T}_q\mathbf{T}|_{z_3\to 0}\right) - 2z\bar{z}\left(\mathbf{T}_{\bar{q}}\mathbf{T} - \mathbf{T}_{\bar{q}}\mathbf{T}|_{z_3\to 0}\right)\right] \tag{64}$$

and

$$\delta^{cc'}\,\tau_5^b(z) = \frac{2\left(Q^2\right)^{1-\varepsilon}}{\pi^{1+\varepsilon}\Gamma[1-\varepsilon]}\frac{(\alpha+z\bar{z})}{\alpha} \times \int_0^{\bar{z}} \mathrm{d}z_3\mathrm{d}^{2+2\varepsilon}\mathbf{q}_2\left[(2z-1+z_3(1+\varepsilon))\left(\mathbf{T}_{\bar{q}}\mathbf{T}\right) - (2\bar{z}-z_3(1+\varepsilon))\left(\mathbf{T}_q\mathbf{T}\right)\right] . \tag{65}$$

After a long calculation we find

$$\begin{aligned}\tau_5^a(z) = \frac{2C_{\mathrm{F}}}{\varepsilon}\int_0^{\bar{z}}\mathrm{d}z_3\left(\frac{2z-1+z_3}{\alpha+z_2\bar{z}_2}\right) &- \frac{1}{N_c}\left(\frac{1}{\varepsilon^2}+\frac{\ln\alpha}{\varepsilon}\right) + 2C_{\mathrm{F}}\Bigg[-\frac{\pi^2}{6} + \int_0^{\bar{z}}\mathrm{d}z_3\left(\frac{2z-1+z_3}{\alpha+z_2\bar{z}_2}\right)\ln\left(\frac{(\alpha+z_2\bar{z}_2)^2}{z_2\bar{z}_2}\right)\Bigg] \\ &+ N_c\int_0^{\bar{z}}\frac{\mathrm{d}z_3}{z_3}\ln\left(\frac{\alpha z^2(\alpha z_2+\bar{z}^2\bar{z}_2)(\alpha+z_2\bar{z}_2)^2}{\bar{z}\bar{z}_2(\alpha\bar{z}_2+zz_3)(\alpha+z\bar{z})^3}\right) \\ &- \frac{1}{N_c}\Bigg[\frac{\ln^2\alpha}{2} + \int_0^{\bar{z}}\mathrm{d}z_3\Bigg\{\ln(\alpha+z_2\bar{z}_2)\left(\frac{\bar{z}}{\alpha+\bar{z}\bar{z}_2}-\frac{z}{\alpha+zz_2}\right) \\ &+ \frac{\bar{z}}{\alpha+\bar{z}\bar{z}_2}\ln\left(\frac{\alpha z_2+\bar{z}^2\bar{z}_2}{\alpha z_3^2\bar{z}_2}\right) + \frac{z}{\alpha+zz_2}\ln\left(\frac{z_3(\alpha\bar{z}_3+zz_2)}{\alpha+z\bar{z}}\right)\Bigg\}\Bigg]\end{aligned} \tag{66}$$

and

$$\begin{aligned}\tau_5^b(z) = -\frac{C_{\mathrm{F}}}{\varepsilon}\int_0^{\bar{z}}\mathrm{d}z_3 &\times\left\{\left(\frac{2z-1+z_3}{\alpha+z_2\bar{z}_2}\right)\frac{\alpha+z\bar{z}}{z\bar{z}} - \frac{z_3-2\bar{z}}{\bar{z}^2}\right\} + N_c\frac{\alpha+z\bar{z}}{\alpha} \\ &\times\int_0^{\bar{z}}\mathrm{d}z_3\ln\left(\frac{\alpha\bar{z}+z_2z_3}{z_2z_3}\right)\left(\frac{2z-1+z_3}{z\bar{z}}+\frac{z_3-2\bar{z}}{\bar{z}^2}\right) \\ &+ \int_0^{\bar{z}}\mathrm{d}z_3\Bigg\{C_{\mathrm{F}}\Bigg[-\frac{\alpha+z\bar{z}}{z\bar{z}}\Bigg(\frac{z_3}{\alpha+z_2\bar{z}_2} + \frac{2z-1+z_3}{\alpha+z_2\bar{z}_2}\ln\left(\frac{(\alpha+z_2\bar{z}_2)^2}{z_2\bar{z}_2}\right)\Bigg) + \frac{z_3}{\bar{z}^2} \\ &+ \frac{2z-1+z_3}{\alpha}\ln\left(\frac{\alpha z_2+\bar{z}^2\bar{z}_2}{\bar{z}z_3}\right)\end{aligned}$$

$$+ \frac{(\alpha+z\bar z)(2z-1+z_3)}{\alpha z\bar z}$$
$$\times \ln\left(\frac{\bar z(\alpha\bar z_2+zz_3)(\alpha z_2+\bar z z_3)}{z_3(\alpha+z\bar z)(\alpha z_2+\bar z^2\bar z_2)}\right)$$
$$+ \frac{(\alpha+z\bar z)(z_3-2\bar z)}{\bar z^2\alpha}\ln\left(\frac{\alpha z_2^2(\alpha z_2+\bar z z_3)}{\bar z^3 z_3}\right)$$
$$+ \frac{z(z_3-2\bar z)}{\bar z\alpha}\ln\left(\frac{\bar z^3(\alpha\bar z_2+zz_3)}{\alpha z_3 z_2^2(\alpha+z\bar z)}\right)\Bigg]$$
$$-\frac{1}{2N_c}\Bigg[\frac{(\alpha+z\bar z)(2z-1+z_3)}{z\bar z\alpha}$$
$$\times\left(2-\frac{zz_2}{\alpha+zz_2}-\frac{\bar z\bar z_2}{\alpha+\bar z\bar z_2}\right)\ln(\alpha+z_2\bar z_2)$$
$$+\frac{(\alpha+z\bar z)(z_3-2\bar z)}{\bar z^2\alpha}\ln\left(\frac{z_3^3(\alpha z_3+\bar z z_2)}{z_2^3(\alpha z_2+\bar z z_3)}\right)$$
$$+\frac{z(z_3-2\bar z)}{\bar z\alpha}\ln\left(\frac{z_2(\alpha\bar z_3+zz_2)}{z_3(\alpha\bar z_2+zz_3)}\right)$$
$$+\frac{(\alpha+z\bar z)(2z-1+z_3)}{\alpha z\bar z}$$
$$\times\left(\ln\left(\frac{(\alpha+z\bar z)(\alpha z_3+\bar z z_2)(\alpha z_2+\bar z^2\bar z_2)}{\alpha\bar z_2 z_2^2 z_3(\alpha\bar z_2+zz_3)(\alpha z_2+\bar z z_3)}\right)\right.$$
$$+\frac{zz_2}{\alpha+zz_2}\ln\left(\frac{z_3(\alpha\bar z_3+zz_2)}{\alpha+z\bar z}\right)$$
$$\left.\left.\left.+\frac{\bar z\bar z_2}{\alpha+\bar z\bar z_2}\ln\left(\frac{\alpha\bar z_2 z_3^2}{\alpha z_2+\bar z^2\bar z_2}\right)\right)\right]\right\}\,. \tag{67}$$

The integration over $\mathbf{q}_2$ in $\tau_4(z)$ is quite simple and leads to

$$\tau_4(z)=\left(C_{\rm F}+\frac{1}{2N_c}\right)$$
$$\times\left[\frac{2}{\varepsilon^2}+\frac{2\ln\alpha+4\ln z}{\varepsilon}+4\ln\left(\frac{s_0/Q^2}{\alpha+z\bar z}\right)\ln\left(\frac{\alpha+z\bar z}{z}\right)\right.$$
$$+2\ln\alpha\ln\left(\frac{\alpha Q^2}{s_0}\right)-\frac{\pi^2}{3}+\ln^2\alpha$$
$$\left.+4\ln z\ln\left(\frac{(\alpha+z\bar z)^3}{\alpha z\bar z}\right)+2{\rm Li}_2\left(-\frac{z\bar z}{\alpha}\right)\right]\,. \tag{68}$$

For $\tau_5(z)$ a more cumbersome calculation gives

$$\tau_5(z)=\frac{C_{\rm F}}{\varepsilon}\left[\frac{(\alpha-z\bar z)}{2z\bar z}\right.$$
$$\times\left(\frac{(1-2z)}{c}\ln(1+2c-2z)-\ln\left(\frac{\alpha+z\bar z}{\alpha}\right)\right)$$
$$\left.-\frac{3}{2}\right]$$
$$+\frac{1}{N_c}\left[-\frac{1}{\varepsilon^2}-\frac{\ln\alpha}{\varepsilon}\right]$$
$$+N_c\left[-\frac{\pi^2}{6}-\ln^2\alpha+\ln(\alpha z)\ln(\alpha+z\bar z)\right.$$
$$+\ln\left(\frac{\alpha z}{\alpha+z\bar z}\right)\ln\left(\frac{\alpha+z}{\alpha+z\bar z}\right)$$
$$+\frac{1}{2}\ln^2\left(\frac{\alpha z}{\alpha+z\bar z}\right)-\frac{1}{2}\ln^2\left(\frac{z}{\bar z}\right)$$
$$-\frac{(\alpha+z\bar z)}{2\alpha\, z\,\bar z}$$
$$\times\left(z\ln\left(\frac{\alpha}{z}\right)\right.$$
$$\left.+\sqrt{z\,(4\alpha+z)}\,\ln\left(\frac{z+\sqrt{z\,(4\alpha+z)}}{-z+\sqrt{z\,(4\alpha+z)}}\right)\right)$$
$$+2\,{\rm Li}_2\left(\frac{2\,z}{1-2\,c}\right)$$
$$+2\,{\rm Li}_2\left(\frac{2\,z}{1+2\,c}\right)+{\rm Li}_2\left(-\frac{z\bar z}{\alpha}\right)+{\rm Li}_2\left(z-\frac{\alpha}{z}\right)$$
$$\left.-{\rm Li}_2\left(-\frac{z}{\alpha}\right)+{\rm Li}_2\left(-\frac{z^2}{\alpha+z\bar z}\right)\right]$$
$$+C_{\rm F}\left[3-\frac{\pi^2}{3}-2\ln\alpha\ln z+2\ln\left(\frac{\alpha}{z}\right)\ln\left(\frac{\alpha+z\bar z}{z}\right)\right.$$
$$-\frac{1}{2}\ln^2\alpha-\frac{(2-z)\,z}{2\,\bar z\,(\alpha-z)}+\frac{z^2}{2\,\bar z\,(\alpha-z^2)}$$
$$-\frac{(1-2z)\,(\alpha+z\bar z)}{2\,c\,z\,\bar z}\ln(1+2c-2z)$$
$$-\left(\frac{z}{2\,(\alpha-z)}-\frac{(2-z)\,z^2}{2\bar z(\alpha-z)^2}+\frac{1+z}{2\,\bar z}\right)\ln\left(\frac{\alpha}{z}\right)$$
$$+\ln^2\left(\frac{2\,c-1}{2\,z}\right)+\ln^2\left(\frac{1+2\,c}{2\,z}\right)$$
$$+4\ln\left(\frac{1+2\,c-2\,z}{2\,c-1}\right)\ln\left(\frac{1+2\,c-2\,z}{2\,z}\right)$$
$$-2\ln\left(\frac{1+2\,c}{2\,z}\right)\ln\left(\frac{1+2\,c-2\,z}{2\,z}\right)$$
$$-\frac{(\alpha+z\bar z)}{2\,\bar z\,(\alpha+z)}\ln z+\ln z\ln\left(\frac{1+2c-2z}{2c-1+2z}\right)$$
$$-\left(\frac{\alpha}{2\,z\,\bar z}+\frac{z^2}{2\,\bar z\,(\alpha+z)}\right)\ln\left(\frac{\alpha+z\bar z}{\alpha}\right)$$
$$+\frac{(\alpha+z\bar z)}{2\,z\,\bar z}\left(\frac{\ln^2\alpha}{2}+2\ln z\,\ln\left(\frac{\alpha+z\bar z}{\alpha}\right)\right.$$
$$\left.+\ln^2\left(\frac{2\,c-1}{2}\right)+\ln^2\left(\frac{1+2\,c}{2}\right)-\ln^2(\alpha+z\bar z)\right)$$
$$-\ln\left(\frac{1+2\,c}{2\,z}\right)\ln\left(\frac{\alpha+z\bar z}{z^2}\right)$$

$$
-\left(\frac{z^3}{2\,\bar z\,(\alpha-z^2)^2}+\frac{z}{\alpha-z^2}+\frac{5-7\,z}{2\,\bar z}\right)\ln\left(\frac{\alpha+z\bar z}{z}\right)
$$
$$
-\frac{(1-2\,z)\,(\alpha-z\bar z)}{2\,c\,z\,\bar z}\left(\ln z\,\ln\left(\frac{2\alpha+(1-2\,c)\,z}{2\alpha+(1+2\,c)\,z}\right)\right.
$$
$$
-\ln(4\alpha+1)\,\ln\left(\frac{1+2\,c-2\,z}{2\,c-1+2\,z}\right)
$$
$$
\left.+2\,\mathrm{Li}_2\left(\frac{1-2\,c-2\,z}{1+2\,c-2\,z}\right)\right)
$$
$$
+\frac{(1+2\,c-2\,z)\,(\alpha-z\bar z)}{2\,c\,z\bar z}\,\mathrm{Li}_2\left(\frac{2\,z}{1-2\,c}\right)
$$
$$
+\frac{(2c-1+2z)\,(\alpha-z\bar z)}{2\,c\,z\,\bar z}\mathrm{Li}_2\left(\frac{2\,z}{1+2c}\right)\Bigg]
$$
$$
+\frac{1}{N_c}\left[-\frac{1}{2\,z}-\frac{2\,z-z^2}{2\,\bar z\,(\alpha-z)}+\frac{(\alpha+z\bar z)}{z\,\bar z}\ln\alpha\right.
$$
$$
+\frac{1}{2}\ln\left(\frac{(2\,c-1)^2}{4\,\alpha}\right)\ln\left(\frac{2\,c-1}{2\,c+1}\right)
$$
$$
+\frac{c\,(1-2z)\,(\alpha+z\bar z)}{z^2\bar z^2}\ln(1+2c-2z)
$$
$$
+\frac{\alpha\,(1-2z)\,(\alpha+z\bar z)}{4\,z^3\bar z^3}\ln 2\ln(1+2c-2z)
$$
$$
+\left(\frac{7}{4}-\frac{\alpha\,(2-z)}{4z^2\,\bar z^2}-\frac{\alpha^2\,\left(2-4\,z+3\,z^2\right)}{4\,z^3\,\bar z^3}\right)
$$
$$
\times\ln^2(1+2\,c-2\,z)
$$
$$
+\left(\frac{z}{2\bar z\,(\alpha-z)}+\frac{2z^2-z^3}{2\,\bar z\,(\alpha-z)^2}\right)\ln\left(\frac{\alpha}{z}\right)
$$
$$
-\ln(1+2c-2z)\,\ln(2c-1+2z)
$$
$$
-\left(\frac{\alpha^2}{z^3\,\bar z^3}+\frac{\alpha-2\alpha^2}{z^2\,\bar z^2}\right)\ln\alpha\ln z
$$
$$
-\frac{(\alpha+z\bar z)}{4\,z^2\,\bar z^2}\ln(\alpha+z\bar z)
$$
$$
+\left(\frac{3-4\,z}{2\,\bar z}+\frac{\alpha\,(1-2\,z)}{z\,\bar z^2}+\frac{z}{2\,\bar z\,(\alpha-z^2)}\right)
$$
$$
\times\ln\left(\frac{z}{\alpha+z\bar z}\right)
$$
$$
-\frac{(\alpha^2+\alpha z-\bar z z^3)}{2\,\bar z\,z^3}
$$
$$
\times\left(-\frac{\pi^2}{6}-7\ln^2 2-2\ln 2\ln\alpha\right.
$$
$$
-\frac{1}{2}\ln^2\alpha+\mathrm{Li}_2\left(-\frac{z^2}{\alpha+z\bar z}\right)
$$
$$
+\ln^2(2\,c-1)+\ln^2(2\,c+1)-\frac{1}{2}\ln^2 z
$$
$$
-\ln 2\ln(2\,c-1+2\,z)-2\mathrm{Li}_2\left(-\frac{\bar z z}{\alpha}\right)
$$
$$
+4\ln(1+2c-2z)\ln(2c-1+2z)
$$
$$
+\frac{1}{2}\ln^2(2c-1+2z)+\ln\left(\frac{\alpha+z}{\alpha}\right)\ln\left(\frac{\alpha\,z}{\alpha+z\bar z}\right)
$$
$$
-\frac{11}{2}\ln 2\,\ln(\alpha+z\bar z)-2\ln\alpha\ln(\alpha+z\bar z)
$$
$$
-2\ln\bar z\,\ln(\alpha+z\bar z)-\ln z\ln(\alpha+z\bar z)
$$
$$
-\mathrm{Li}_2\left(-\frac{z}{\alpha}\right)+2\mathrm{Li}_2\left(\frac{2\,z}{1-2\,c}\right)
$$
$$
\left.\left.+2\mathrm{Li}_2\left(\frac{2\,z}{1+2\,c}\right)-\mathrm{Li}_2\left(z-\frac{\alpha}{z}\right)\right)\right]\,. \tag{69}
$$

Equations (60), (61), (68) and (69) give the result for the $(q\bar q g)$ contribution to the impact factor.

4.3 The result for NLA impact factor

Now we are ready to add together the $(q\bar q)$ and the $(q\bar q g)$ contributions and to obtain (as anticipated above), after the treatment of the ultraviolet and of the collinear singularities, the finite result for the NLA impact factor.

In the sum of all contributions – the $z\leftrightarrow\bar z$ symmetry was used where necessary – we find

$$
\sum_{i=1,\dots,5}\tau_i(z)=\frac{C_{\rm F}}{\varepsilon}
\times\left[\frac{3}{2}+\frac{(1-2\,z)\,(\alpha-\bar z z)}{4\,c\,\bar z\,z}\ln\left(\frac{1+2\,c-2\,z}{2\,c-1+2\,z}\right)\right.
-\frac{(\alpha+\bar z z)}{4\,c\,\bar z\,z}\ln\left(\frac{2\,c+1}{2\,c-1}\right)
\left.-\frac{(\alpha-\bar z z)}{2\,\bar z\,z}\ln\left(\frac{\alpha+\bar z z}{\alpha}\right)\right]-\frac{\beta_0}{2\,\varepsilon}+\dots\,, \tag{70}
$$

where the ellipsis stand for the terms which are finite for $\varepsilon\to 0$. First of all, we note that the double poles in ε which appear due to soft singularities and are present in the separate contributions cancel out in the sum (70). What is left are the single poles in ε which represent the ultraviolet and the collinear singularities which are removed by the renormalization of the strong coupling constant and of the distribution amplitude, as explained in Sect. 2.

After substituting the bare strong coupling constant and the meson distribution amplitude by the renormalized quantities, given respectively in (15) and (17), we find the following expressions for the ultraviolet

$$
\Delta^{\alpha_s}\,T_{\rm H}(z)=\frac{\alpha_s(\mu_{\rm R})}{4\pi}\beta_0\left[\frac{1}{\hat\varepsilon}+\ln\left(\frac{\mu_{\rm R}^2}{\mu^2}\right)\right]T_{\rm H}^{(0)}(z)\,, \tag{71}
$$

and the collinear

$$
\Delta^{\rm coll}\,T_{\rm H}(z) \tag{72}
$$

$$= -\frac{\alpha_s(\mu_F)}{2\pi}\left[\frac{1}{\hat{\varepsilon}} + \ln\left(\frac{\mu_F^2}{\mu^2}\right)\right]\int_0^1 du\, T_H^{(0)}(u)\, V^{(1)}(u,z)\ ,$$

counterterms to T_H, where the LLA hard-scattering amplitude $T^{(0)}$ and the one-loop evolution kernel $V^{(1)}$ are given by (29) and (13), respectively. Calculating the integral in (72) and then combining the corresponding contributions coming from the counterterms with the singular part of (70), we see that the ultraviolet and the collinear singularities in the hard-scattering amplitude cancel and the result for the finite part may be presented as in (70) with the replacements

$$\frac{\beta_0}{\varepsilon} \to \beta_0 \ln\left(\frac{Q^2}{\mu_R^2}\right)\ , \qquad \frac{C_F}{\varepsilon} \to C_F \ln\left(\frac{Q^2}{\mu_F^2}\right)\ . \tag{73}$$

Finally we find that the NLA impact factor is given by (5) with

$$T_H(z,\alpha,s_0,\mu_F,\mu_R)| \tag{74}$$
$$= \alpha_s(\mu_R)\frac{\alpha}{\alpha+z\bar{z}}\left\{1+\frac{\alpha_s(\mu_R)}{4\pi}\left[\tau(z)+\tau(\bar{z})\right]\right\}\ ,$$

where

$$\begin{aligned}
\tau(z) &= C_F \ln\left(\frac{Q^2}{\mu_F^2}\right) \\
&\times\left[\frac{3}{2} + \frac{(1-2\,z)\,(\alpha-\bar{z}z)}{4\,c\,\bar{z}\,z}\ln\left(\frac{1+2\,c-2\,z}{2\,c-1+2\,z}\right)\right. \\
&-\frac{(\alpha+\bar{z}z)}{4\,c\,\bar{z}\,z}\ln\left(\frac{2\,c+1}{2\,c-1}\right) \\
&\left.-\frac{(\alpha-\bar{z}z)}{2\,\bar{z}\,z}\ln\left(\frac{\alpha+\bar{z}z}{\alpha}\right)\right] - \frac{\beta_0}{2}\ln\left(\frac{Q^2}{\mu_R^2}\right) \\
&+n_f\left[-\frac{5}{9}+\frac{\ln\alpha}{3}\right] + C_F\left[-\frac{\ln^2\alpha}{2} - 3\ln\left(\frac{\alpha+\bar{z}z}{z}\right)\right. \\
&+4\ln^2\left(c-z+\frac{1}{2}\right) - 2\ln\left(c-\frac{1}{2}\right)\ln\left(c+\frac{1}{2}\right) \\
&+\frac{(\alpha+\bar{z}z)}{2\,\alpha\,\bar{z}\,z}\left(\ln\alpha + 2\,c\ln\left(\frac{2\,c+1}{2\,c-1}\right)\right) \\
&-\frac{(1-2\,z)\,(\alpha+\bar{z}z)}{2\,c\,\bar{z}\,z}\ln(1+2\,c-2\,z) \\
&-\frac{(\alpha+\bar{z}z)}{2\,\bar{z}\,z}\ln\left(\frac{\alpha+\bar{z}z}{\alpha}\right) + \frac{(\alpha+\bar{z}z)}{\bar{z}\,(\alpha+z)}\ln\left(\frac{\alpha+\bar{z}z}{\alpha\,z}\right) \\
&+\frac{(\alpha+\bar{z}z)}{2\,c\,\bar{z}\,z} \\
&\times\left(\frac{\pi^2}{6} + \ln 4\ln\alpha + \frac{1}{2}\ln\left(\frac{1+2\,c}{2\,c-1}\right)\right. \\
&+2\ln c\ln\left(\frac{2\,c-1}{4}\right) - \ln^2(2\,c+1) \\
&-\ln^2 c + \frac{1}{4}\ln^2\left(\frac{2\,c+1}{2\,c-1}\right) - 2\mathrm{Li}_2\left(\frac{2\,c-1}{4\,c}\right) \\
&\left.-\mathrm{Li}_2\left(\frac{2}{1+2\,c}\right)\right) \\
&+\frac{(\alpha+\bar{z}z)}{2\,\bar{z}\,z}\left(\frac{\ln^2\alpha}{2} - 2\ln\left(c-\frac{1}{2}\right)\ln\left(c+\frac{1}{2}\right)\right. \\
&+\ln^2\left(\frac{z}{\alpha}\right) - \ln^2\left(\frac{\alpha+\bar{z}z}{z}\right) + 2\mathrm{Li}_2\left(\frac{2\,z}{1-2\,c}\right) \\
&\left.+2\mathrm{Li}_2\left(\frac{2\,z}{1+2\,c}\right)\right) \\
&-\frac{(1-2\,z)\,(\alpha-\bar{z}z)}{2\,c\,\bar{z}\,z} \\
&\times\left(\ln\left(\frac{z}{4\alpha+1}\right)\ln\left(\frac{2\alpha+(1-2\,c)\,z}{2\alpha+(1+2\,c)\,z}\right)\right. \\
&-\ln(4\alpha+1)\ln\left(\frac{2\,c+1}{2\,c-1}\right) + 2\mathrm{Li}_2\left(\frac{1-2\,c-2\,z}{1+2\,c-2\,z}\right) \\
&\left.\left.-\mathrm{Li}_2\left(\frac{2\,z}{1-2\,c}\right) + \mathrm{Li}_2\left(\frac{2\,z}{1+2\,c}\right)\right)\right] \\
&+N_c\left[\ln\left(s_0/Q^2\right)\ln\left(\frac{(\alpha+\bar{z}z)^2}{z^2\alpha}\right)\right. \\
&+\frac{20}{9} - \frac{\ln\alpha}{3} + \frac{1}{2}\ln^2\left(\frac{\bar{z}}{z}\right) \\
&+\frac{1}{2}\ln^2\left(\frac{\alpha+\bar{z}z}{\alpha}\right) - 2\ln\left(\frac{\alpha+z}{z}\right)\ln\left(\frac{\alpha+\bar{z}z}{\alpha\,z}\right) \\
&-\ln^2\left(\frac{\alpha+\bar{z}z}{z}\right) + 3\ln z\ln\left(\frac{\alpha+\bar{z}z}{\alpha\,z}\right) + 2\ln^2 z \\
&-\frac{(\alpha+\bar{z}z)}{2\,\alpha\,\bar{z}\,z}\left(z\ln\left(\frac{\alpha}{z}\right)\right. \\
&\left.+\sqrt{z\,(4\,\alpha+z)}\ln\left(\frac{z+\sqrt{z\,(4\,\alpha+z)}}{-z+\sqrt{z\,(4\,\alpha+z)}}\right)\right) \\
&+\mathrm{Li}_2\left(\frac{2\,z}{1-2\,c}\right) + \mathrm{Li}_2\left(\frac{2\,z}{1+2\,c}\right) + 2\mathrm{Li}_2\left(-\frac{z^2}{\alpha+\bar{z}z}\right) \\
&\left.-2\mathrm{Li}_2\left(-\frac{z}{\alpha}\right) + 3\,\mathrm{Li}_2\left(-\frac{\bar{z}z}{\alpha}\right)\right] \\
&+\frac{1}{N_c}\left[\frac{5}{2} + \left(\frac{\alpha+\bar{z}z}{\bar{z}\,z} - \frac{3}{2}\right)\ln\alpha\right. \\
&+\frac{1}{2}\ln\left(\frac{4\,\alpha}{(2\,c-1)^2}\right)\ln\left(\frac{2\,c+1}{2\,c-1}\right) \\
&+\frac{1}{2}\ln^2\left(\frac{1+2\,c-2\,z}{2\,c-1+2\,z}\right) \\
&+\frac{c\,(1-2\,z)\,(\alpha+\bar{z}z)}{\bar{z}^2\,z^2}\ln(1+2\,c-2\,z) \\
&+\frac{(1-2\,z)\,(\alpha+\bar{z}z)}{\bar{z}^2 z}\ln\left(\frac{z}{\alpha+\bar{z}z}\right) + \mathrm{Li}_2\left(\frac{2\,z}{1+2\,c}\right) \\
&+\ln z\ln\left(\frac{\alpha+\bar{z}z}{\alpha}\right)
\end{aligned}$$

$$
\begin{aligned}
&+\frac{(\alpha+\bar z z)}{4\,\bar z^2 z^2}\\
&\times\left(2\,c\,\ln\left(\frac{2\,c+1}{2\,c-1}\right)-\ln\left(\frac{\alpha+\bar z z}{\alpha}\right)\right)+\mathrm{Li}_2\left(\frac{2\,z}{1-2\,c}\right)\\
&-\frac{(\alpha^2+\alpha\,z-\bar z\,z^3)}{2\,\bar z\,z^3}\\
&\times\left(2\ln\left(c-z+\frac12\right)\ln\left(c+z-\frac12\right)\right.\\
&-2\ln\left(c-\frac12\right)\ln\left(c+\frac12\right)\\
&+\ln\left(\frac{2\,c+1}{2\,c-1}\right)\ln\left(\frac{2\,\alpha+(1+2\,c)\;z}{2\,\alpha+(1-2\,c)\;z}\right)\\
&-\ln\left(\frac{\alpha\,\bar z^2\,z^2}{(\alpha+\bar z z)^2}\right)\ln\left(\frac{\alpha+\bar z z}{\alpha}\right)\\
&+2\ln\left(\frac{\alpha+z}{\alpha}\right)\ln\left(\frac{\alpha\,z}{\alpha+\bar z z}\right)\\
&-2\mathrm{Li}_2\left(-\frac{z}{\alpha}\right)+4\mathrm{Li}_2\left(\frac{2\,z}{1-2\,c}\right)+4\mathrm{Li}_2\left(\frac{2\,z}{1+2\,c}\right)\\
&\left.\left.-\,2\mathrm{Li}_2\left(-\frac{\bar z z}{\alpha}\right)+2\mathrm{Li}_2\left(-\frac{z^2}{\alpha+\bar z z}\right)\right)\right]\,. \qquad (75)
\end{aligned}
$$

Equations (5), (74) and (75) represent the main result of the present paper.

In LLA terms of the type $\sim\alpha_{\mathrm s}^n\ln^n(s/s_0)$ are summed. Therefore the leading energy scale uncertainty of a LLA amplitude is related with the contributions $\sim\alpha_{\mathrm s}^n\ln^{n-1}(s)\ln(s_0)$. These terms represent some particular part of NLA correction to the amplitude. Note that in the sum of all NLA terms the contributions $\sim\alpha_{\mathrm s}^n\ln^{n-1}(s)\ln(s_0)$ should cancel, since by construction a NLA amplitude does not depend on s_0 with the NLA accuracy.

Using our result for the meson impact factor let us demonstrate the cancellation of the $\sim\alpha_{\mathrm s}^n\ln^{n-1}(s)\ln(s_0)$ contributions to the forward amplitude of the process of two ρ mesons production, $\gamma_1^*(Q_1^2)\gamma_2^*(Q_2^2)\to\rho_1\rho_2$. Examining (1) one can see that the contributions of such a type cannot be generated by the corrections to the kernel of BFKL equation, since these corrections do not depend on s_0. Therefore, for our purposes, we can use the known result for the Green's function in the LLA approximation. In the azimuth symmetric, $n=0$, sector it reads

$$
G_\omega(\mathbf q_1,\mathbf q_2,\mathbf\Delta=0)=\int\limits_{-\infty}^{+\infty}\frac{\mathrm d\nu}{2\pi^2}\,\frac{(\mathbf q_1^{\,2})^{\frac12+\mathrm i\nu}(\mathbf q_2^{\,2})^{\frac12-\mathrm i\nu}}{\omega-\bar\alpha_{\mathrm s}\chi(\nu)} \qquad (76)
$$

where

$$
\bar\alpha_{\mathrm s}=\frac{\alpha_{\mathrm s}N_c}{\pi}\,, \qquad (77)
$$

$$
\chi(\nu)=2\Psi(1)-\Psi\left(\frac12+\mathrm i\nu\right)-\Psi\left(\frac12-\mathrm i\nu\right)\,,
$$

and $\Psi(x)=\Gamma'(x)/\Gamma(x)$. Inserting (76) in (1) we found the following representation for the amplitude

$$
\mathrm{Im}_s(\mathcal A)^{\rho_1\rho_2}_{\gamma_1^*\gamma_2^*}=\frac{s}{(2\pi)^2}\int\limits_{-\infty}^{+\infty}\mathrm d\nu\left(\frac{s}{s_0}\right)^{\bar\alpha_{\mathrm s}\chi(\nu)}I_1(\nu,s_0)I_2(\nu,s_0)\,; \qquad (78)
$$

here

$$
\begin{aligned}
I_1(\nu,s_0)&=\int\mathrm d^2q_1\,\frac{(\mathbf q_1^{\,2})^{\mathrm i\nu-\frac32}}{\sqrt{2}\pi}\,\Phi_{\gamma_1^*\to\rho_1}(\mathbf q_1^{\,2},s_0)\,,\\
I_2(\nu,s_0)&=\int\mathrm d^2q_2\,\frac{(\mathbf q_2^{\,2})^{-\mathrm i\nu-\frac32}}{\sqrt{2}\pi}\,\Phi_{\gamma_2^*\to\rho_2}(\mathbf q_2^{\,2},s_0)\,. \qquad (79)
\end{aligned}
$$

According to our calculation

$$
\begin{aligned}
&\Phi_{\gamma_{\mathrm L}^*\to\rho_{\mathrm L}}\left(\alpha=\frac{\mathbf q^{\,2}}{Q^2},s_0\right)\\
&=-\frac{4\pi e f_\rho\delta^{cc'}}{\sqrt2 N_cQ}\int\limits_0^1\mathrm dz\,\phi_\|(z)\,\alpha_{\mathrm s}\frac{\alpha}{\alpha+z\bar z} \qquad (80)\\
&\times\left[1+\frac{\bar\alpha_{\mathrm s}}{4}\ln(s_0)\ln\left(\frac{(\alpha+z\bar z)^4}{\alpha^2z^2\bar z^2}\right)+\dots\right]\,;
\end{aligned}
$$

the ellipsis in (80) stand for the NLA contributions to the impact factor which do not depend on s_0. Performing the integration over reggeon momenta in (79) we found that

$$
\begin{aligned}
&I_{1,2}(\nu,s_0)\sim(Q_{1,2}^2)^{\pm\mathrm i\nu-1}J(\pm\nu)\\
&\times\int\limits_0^\infty\mathrm dy\frac{y^{\pm\mathrm i\nu-\frac12}}{y+1}\left[1+\frac{\bar\alpha_{\mathrm s}}{2}\ln(s_0)\ln\left(\frac{(y+1)^2}{y}\right)+\dots\right]\\
&=(Q_{1,2}^2)^{\pm\mathrm i\nu-1}J(\pm\nu) \qquad (81)\\
&\times\frac{\pi}{\cosh(\pi\nu)}\left[1+\frac{\bar\alpha_{\mathrm s}\chi(\nu)}{2}\ln(s_0)+\dots\right]\,,
\end{aligned}
$$

where

$$
J(\nu)=\int\limits_0^1\mathrm dz\,\phi_\|(z)\,(z\bar z)^{\mathrm i\nu-\frac12}\,. \qquad (82)
$$

Thus we obtain that

$$
\begin{aligned}
&\mathrm{Im}_s(\mathcal A)^{\rho_1\rho_2}_{\gamma_1^*\gamma_2^*}\\
&\sim\frac{sf_\rho^2}{Q_1^2Q_2^2}\int\limits_{-\infty}^{+\infty}\mathrm d\nu J(\nu)J(-\nu)\left(\frac{Q_1^2}{Q_2^2}\right)^{\mathrm i\nu}\frac{\pi^2}{\cosh^2(\pi\nu)}\\
&\times\left(\frac{s}{s_0}\right)^{\bar\alpha_{\mathrm s}\chi(\nu)}\left[1+\frac{\bar\alpha_{\mathrm s}\chi(\nu)}{2}\ln(s_0)+\dots\right]^2\,. \qquad (83)
\end{aligned}
$$

Expanding in series the last line of (83), one can easily see that the dependence of the amplitude on s_0 indeed cancels with the NLA accuracy. This calculation shows that the s_0

dependence of our result for the impact factor is consistent with the form of the BFKL kernel.

The hard-scattering amplitude in the limits of small and large virtualities of the reggeized gluon reads

$$\begin{aligned}
&T_{\rm H}(z,\alpha,s_0,\mu_{\rm F},\mu_{\rm R})|_{\alpha\to 0}\\
&= \alpha_s(\mu_{\rm R})\frac{\alpha}{z\bar z}\left[1+\frac{\alpha_s(\mu_{\rm R})}{4\pi}\left(n_f\left[-\frac{10}{9}+\frac{2\ln\alpha}{3}\right]\right.\right.\\
&\quad -\beta_0\ln\left(\frac{Q^2}{\mu_{\rm R}^2}\right)\\
&\quad +N_c\left[\frac{67}{9}+\frac{\ln\alpha}{3}-\ln^2\alpha\right.\\
&\quad -3\ln(z\bar z)+2\ln\left(\frac{s_0}{Q^2}\right)\ln\left(\frac{z\bar z}{\alpha}\right)\\
&\quad \left.-\frac{5\pi^2}{6}+\ln^2 z+\ln^2\bar z+\ln z\ln\bar z\right]\\
&\quad +C_{\rm F}\left[2z\ln\bar z+2\bar z\ln z-\frac{\pi^2}{3}\right.\\
&\quad +z\ln^2\bar z+\bar z\ln^2 z-8-2\ln\alpha+2\,z\,{\rm Li}_2(z)\\
&\quad +2\,\bar z\,{\rm Li}_2(\bar z)\\
&\quad \left.\left.\left.+(3+2z\ln\bar z+2\bar z\ln z)\ln\left(\frac{Q^2}{\mu_{\rm F}^2}\right)\right]\right)\right]\\
&\quad +\mathcal{O}\left(\alpha_s^2(\mu_{\rm R})\,\alpha^2\right)\ ; \qquad (84)
\end{aligned}$$

$$\begin{aligned}
&T_{\rm H}(z,\alpha,s_0,\mu_{\rm F},\mu_{\rm R})|_{\alpha\to \infty}\\
&= \alpha_s(\mu_{\rm R})\left[1+\frac{\alpha_s(\mu_{\rm R})}{4\pi}\left(n_f\left[-\frac{10}{9}+\frac{2\ln\alpha}{3}\right]\right.\right.\\
&\quad -\beta_0\ln\left(\frac{Q^2}{\mu_{\rm R}^2}\right) \qquad (85)\\
&\quad +N_c\left[\frac{22}{9}-\frac{20\ln\alpha}{3}-2\ln^2\alpha-\frac{\ln\bar z}{2\,z}-\frac{\ln z}{2\,\bar z}\right.\\
&\quad +3\ln(z\bar z)+2\ln\left(\frac{s_0}{Q^2}\right)\ln\left(\frac{\alpha}{z\bar z}\right)+4\ln\alpha\ln(z\bar z)\\
&\quad \left.\left.\left.-2\ln z\ln\bar z-3\ln^2 z-3\ln^2\bar z\right]\right)\right]+\mathcal{O}\left(\frac{\alpha_s^2(\mu_{\rm R})}{\alpha}\right)\ .
\end{aligned}$$

These limiting expressions may be useful for the analysis of vector meson production amplitudes in the asymmetric kinematics, when the two virtualities are essentially different, $Q_1 \gg Q_2$. In this case not only a large $\ln(s)$, but also large $\ln(Q_1^2/Q_2^2)$ appear in the perturbative expansion. In the BFKL approach powers of the logarithm of virtuality originate from the region of reggeon momenta where $Q_1^2 \gg \mathbf{q}^{\,2} \gg Q_2^2$, which corresponds to the limits (84), (85) for the meson impact factor.

5 Summary and conclusions

In this paper we have considered the impact factor for the virtual photon to light vector meson transition in the case of the dominant longitudinal polarization. We have shown that, up to power suppressed corrections, both in the leading and in the next-to-leading approximation the expression for the impact factor factorizes into the convolution of a perturbatively calculable hard-scattering amplitude $T_{\rm H}$ and a meson twist-2 distribution amplitude. We have determined $T_{\rm H}$ in the next-to-leading order by calculating cut diagrams with effectively no more than two-particle intermediate states. We have observed cancellation of the soft infrared divergences between the "real" and the "virtual" parts of the radiative corrections. Collinear infrared divergences have been absorbed into the definition of the distribution amplitude. We have obtained finally a close analytical expression for the impact factor which can be used, after convolution with the Green's function of two interacting reggeized gluons, to build entirely within perturbative QCD the complete amplitude for a physical process, in the next-to-leading logarithmic approximation.

This result can have important theoretical implications, since it could shed light on the correct choice of energy scales in the BFKL approach and could be used to compare different approaches such as BFKL and DGLAP. Moreover, it can be considered as the first step towards the study of phenomenologically relevant processes, such as the vector meson electroproduction at the HERA collider and the production of two mesons in the photon collision which can be studied at high-energy e^+e^- and $e\gamma$ colliders.

This work was completed after M.I. Kotsky tragically passed away. We had the pleasure to know him not only as a bright scientist, but also as an exceptionally rich personality. We missed a friend.

Acknowledgements. We thank V.S. Fadin for many stimulating discussions. D.I. thanks the Dipartimento di Fisica dell'Università della Calabria and the Istituto Nazionale di Fisica Nucleare (INFN), Gruppo collegato di Cosenza, for the warm hospitality while part of this work was done and for the financial support. The work of D.I. was supported also by the Alexander von Humboldt Foundation and by RFBR 03-02-17734.

References

1. V.S. Fadin, E.A. Kuraev, L.N. Lipatov, Phys. Lett. B **60**, 50 (1975); E.A. Kuraev, L.N. Lipatov, V.S. Fadin, Zh. Eksp. Teor. Fiz. **71**, 840 (1976) [Sov. Phys. JETP **44**, 443 (1976)]; **72**, 377 (1977) [**45**, 199 (1977)]; Ya.Ya. Balitskii, L.N. Lipatov, Sov. J. Nucl. Phys. **28**, 822 (1978)
2. A.M. Cooper-Sarkar, R.C.E. Devenish, A. De Roeck, Int. J. Mod. Phys. A **13**, 3385 (1998), and references therein
3. V.S. Fadin, R. Fiore, Phys. Lett. B **440**, 359 (1998)
4. L.N. Lipatov, V.S. Fadin, Sov. J. Nucl. Phys. **50**, 712 (1989)
5. V.S. Fadin, R. Fiore, M.I. Kotsky, Phys. Lett. B **359**, 181 (1995)
6. V.S. Fadin, R. Fiore, M.I. Kotsky, Phys. Lett. B **387**, 593 (1996)

7. V.S. Fadin, L.N. Lipatov, Nucl. Phys. B **406**, 259 (1993)
8. V.S. Fadin, R. Fiore, A. Quartarolo, Phys. Rev. D **50**, 5893 (1994); V.S. Fadin, R. Fiore, M.I. Kotsky, Phys. Lett. B **389**, 737 (1996); V.S. Fadin, L.N. Lipatov, Nucl. Phys. B **477**, 767 (1996); V.S. Fadin, M.I. Kotsky, L.N. Lipatov, Phys. Lett. B **415**, 97 (1997); V.S. Fadin, R. Fiore, A. Flachi, M.I. Kotsky, Phys. Lett. B **422**, 287 (1998)
9. S. Catani, M. Ciafaloni, F. Hautman, Phys. Lett. B **242**, 97 (1990); Nucl. Phys. B **366**, 135 (1991); G. Camici, M. Ciafaloni, Phys. Lett. B **386**, 341 (1996); Nucl. Phys. B **496**, 305 (1997)
10. V.S. Fadin, L.N. Lipatov, Phys. Lett. B **429**, 127 (1998)
11. G. Camici, M. Ciafaloni, Phys. Lett. B **430**, 349 (1998)
12. V.S. Fadin, R. Fiore, M.I. Kotsky, A. Papa, Phys. Rev. D **61**, 094005 (2000); Phys. Rev. D **61**, 094006 (2000)
13. M. Ciafaloni, D. Colferai, Nucl. Phys. B **538**, 187 (1999)
14. J. Bartels, D. Colferai, G.P. Vacca, Eur. Phys. J. C **29**, 235 (2003)
15. J. Bartels, D. Colferai, S. Gieseke, A. Kyrieleis, Phys. Rev. D **66**, 094017 (2002)
16. V.S. Fadin, D.Yu. Ivanov, M.I. Kotsky, Nucl. Phys. B **658**, 156 (2003)
17. V.S. Fadin, A.D. Martin, Phys. Rev. D **60**, 114008 (1999)
18. V.L. Chernyak, A.R. Zhitnitsky, JETP Lett. **25**, 510 (1977); Yad. Fiz. **31**, 1053 (1980); V.L. Chernyak, V.G. Serbo, A.R. Zhitnitsky, JETP Lett. **26**, 594 (1977); Sov. J. Nucl. Phys. **31**, 552 (1980)
19. G.P. Lepage, S.J. Brodsky, Phys. Lett. B **87**, 359 (1979); Phys. Rev. Lett. **43**, 545, 1625 (E) (1979); Phys. Rev. D **22**, 2157 (1980); S.J. Brodsky, G.P. Lepage, A.A. Zaidi, Phys. Rev. D **23**, 1152 (1981)
20. A.V. Efremov, A.V. Radyushkin, Phys. Lett. B **94**, 245 (1980); Teor. Mat. Fiz. **42**, 147 (1980)
21. P. Ball, V.M. Braun, Y. Koike, K. Tanaka, Nucl. Phys. B **529**, 323 (1998)
22. I.F. Ginzburg, D.Yu. Ivanov, Phys. Rev. D **54**, 5523 (1996)
23. D.Yu. Ivanov, R. Kirschner, Phys. Rev. D **58**, 114026 (1998)
24. D.Yu. Ivanov, R. Kirschner, A. Schäfer, L. Szymanowski, Phys. Lett. B **478**, 101 (2000) [Erratum B **498**, 295 (2001)]
25. V.S. Fadin, D.Yu. Ivanov, M.I. Kotsky, Phys. Atom. Nucl. **65**, 1513 (2002) [Yad. Fiz. **65**, 1551 (2002)]
26. V.S. Fadin, R. Fiore, A. Quartarolo, Phys. Rev. D **50**, 2265 (1994)